A Review of Satellite-Derived Figures of the Geoid and Their Geophysical Significance[1]

GEORGE P. WOOLLARD[2] and MOHAMMAD ASADULLAH KHAN[2]

ONE OF THE MAJOR GEODETIC RESULTS that has come out of the satellite tracking program, in addition to the revision of the degree of polar flattening for the Earth, is that the Earth is characterized by a series of previously undefined geoidal *highs* and *lows*. As these cannot be correlated with the surface mass distribution defined by the continents and ocean basins, they presumably are related to regional variations in gravity resulting from the mass distributions within the Earth. That they may have other geophysical as well as geological significance has been proposed by various investigators (Lee and MacDonald, 1963; Wang, 1963; Runcorn, 1964; Baussus, 1960; Vogel, 1960; Scheffer, 1966; Strange, 1966). However, the geoidal pattern defined by different investigators has not been totally consistent in that there are differences both in basic pattern and in magnitude of the geoidal undulations. There has also been an evolutionary trend in the complexity of the geoidal pattern defined. This change in overall pattern, as well as the differences in pattern obtained by different investigators, can be related to the sampling of data used (number of satellites and their orbital elements as well as number and distribution of tracking stations); the type of tracking data used (optical versus electronic doppler observations); the parameters of the reference ellipsoid used (particularly the degree of polar flattening); the degree of fit as represented by the order and degree of the coefficient terms and their derived values; and the combinations of data used, such as satellite plus surface gravity observations. There have also been studies based entirely on surface gravity observations which have been influenced in various degrees by the assumptions made by different

investigators for the surface gravity field where there are no observational data.

In approaching the problem of how best to determine the geophysical significance of the geoidal results published to date, Kaula (1966, 1967) adopted a statistical approach based on a cross-covariance analysis. The authors (Khan and Woollard, 1968a) undertook a somewhat different approach and computed a series of geoidal maps based on various combinations of zonal and tesseral harmonic coefficients derived by various investigators, as well as maps based on mean coefficient values, and these results were then used to compute the anomalous gravity field so that direct comparisons could be made with actual free air gravity anomalies and other geophysical data. The present paper reviews: (a) the geoidal results obtained by various investigators, (b) the derived gravity field and its relation to the surface gravity field, and (c) the geophysical and geological relations in two areas of anomalous geoidal height.

REVIEW OF SATELLITE-DERIVED FIGURES FOR THE GEOID

One of the early geoidal maps derived from satellite data was that by Kaula (1963) using optical observations and based on five satellites. This is shown in Figure 1. In the Western Hemisphere (180° to 0° West longitude) only one anomalous closure in geoidal height is defined, that of +30 meters in the South Atlantic Ocean and centered at about 10° West longitude, 45° South latitude. In the Eastern Hemisphere (0° to 180° East longitude) there are four closures. Two of these represent major departures in geoidal height. One has a negative closure of about —50 meters and is centered at about 70° East longitude, 10° North latitude in the Indian Ocean. The other has a positive closure of about +50 meters and is centered at about 150° East longitude, 10° South latitude in the New Guinea-Solo-
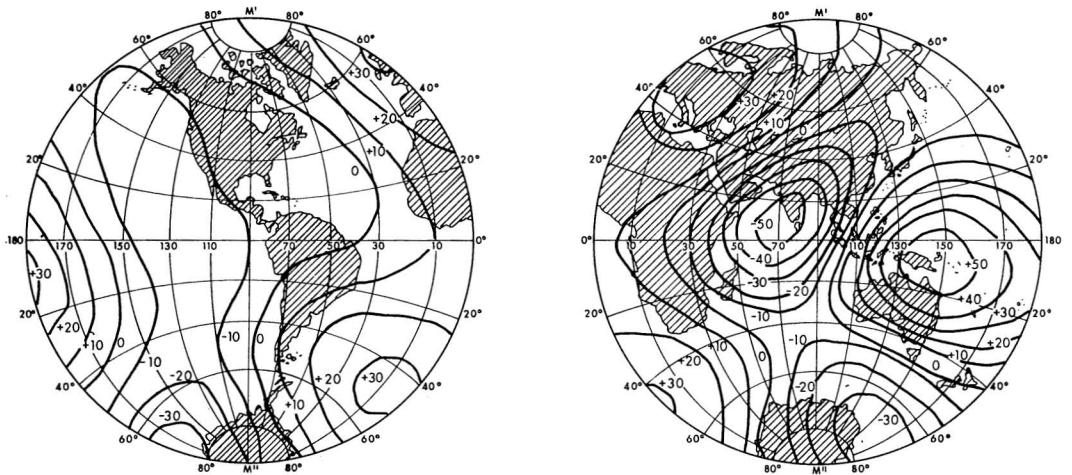
FIG. 1. Geoid based on optical data for five satellites (Kaula, 1963). *Left,* Western Hemisphere, 180°W to 0°; *right,* Eastern Hemisphere, 0° to 180° E.

mon Islands area. Of the other two closures, one is positive (about +30 meters) and is centered over western Europe, and the other is negative (about —30 meters) and is centered somewhat north of the Ross Sea off Antarctica.

Figure 2 is a similar early geoidal map derived by Guier (1963) using doppler tracking data. This agrees closely with Figure 1 for the two areas of pronounced geoidal anomaly in the Eastern Hemisphere in that it shows a +62 meter closure just north of New Guinea and a

—76 meter closure in the Indian Ocean. However, there is a lack of agreement with the other closures shown in Figure 1. There is a positive closure of +64 meters centered over the western Mediterranean Sea, a +46 meter closure between the tip of South Africa and Antarctica, and a pronounced negative closure of —50 meters centered over the Bahama Islands off the east coast of North America.

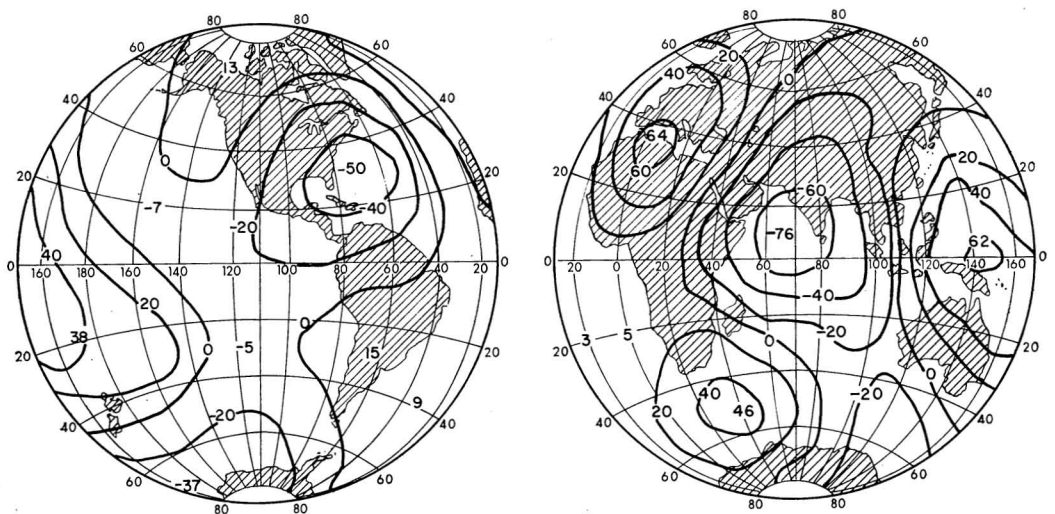Both Figures 1 and 2 represented low order degrees of fit to the data, and both were re-

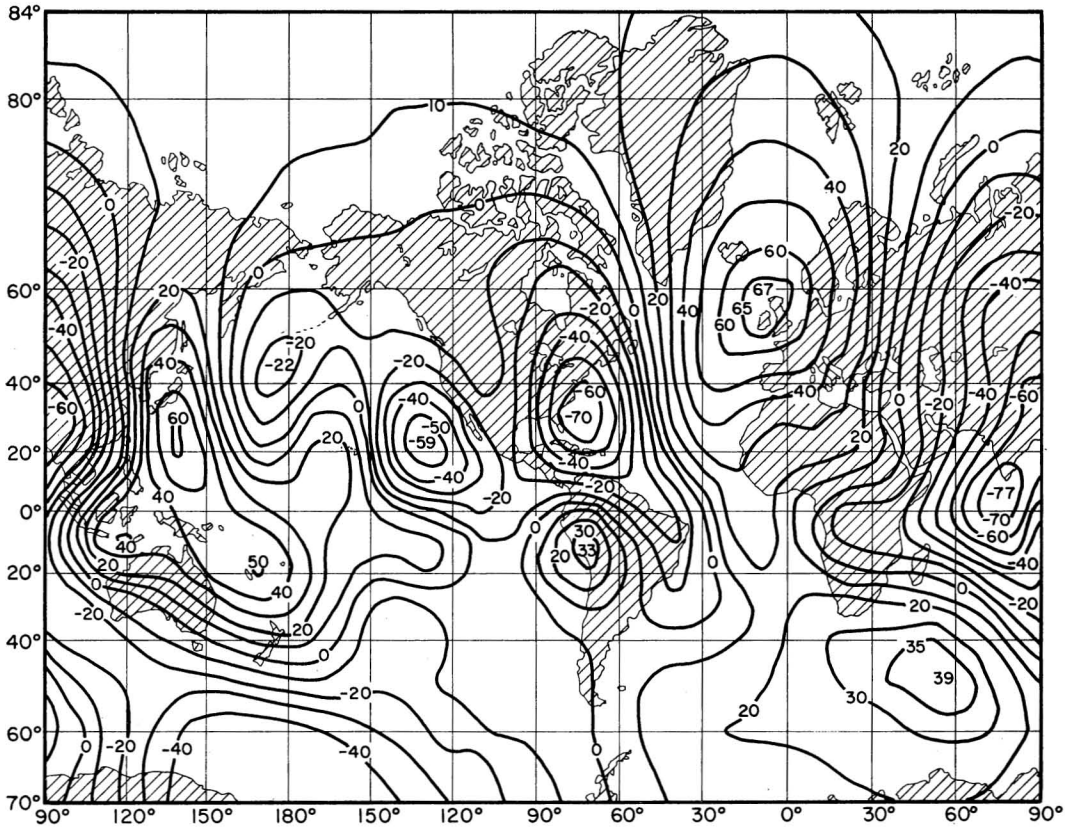FIG. 2. Geoid based on doppler data for three satellites (Guier, 1963).

stricted in terms of the orbital elements (height and inclination) of the first satellites. The differences in results can be attributed to the differences in tracking station locations, the differences in type of data, and the differences in assumptions made in carrying out the harmonic analysis of the data.

If more recent maps of the geoid are examined which are based on more abundant data involving a larger number of satellites with more variable orbital elements and with higher degrees of fit, it is seen that the geoid appears to be extremely complex. Figure 3 is a geoidal map prepared by Izsak (1967) based on optical tracking data for 11 satellites. It has certain points in common with Figure 1 in that the geoidal *low* in the Indian Ocean and the geoidal *high* in the New Guinea-Solomon Islands region are duplicated, but with somewhat magnified values (−73 meters in the Indian Ocean and +63 meters in the Solomon Islands region), and certain differences. The most pronounced changes are: (a) the shift of the geoidal *high* from western Europe to the western North Atlantic region with a value of +43 meters off the British Isles, (b) the shift of the geoidal *low* from the Ross Sea area off Antarctica to the region off southwestern Australia with a value of −42 meters, and (c) the shift of the geoidal *high*

in the South Atlantic area to the region between South Africa and Antarctica with a value of +49 meters. In addition to the above, Izsak's (1967) results indicate several new areas of geoidal anomaly: (a) a geoidal *low* of −23 meters centered at about 15° North latitude, 50° West longitude in the western Atlantic Ocean off the Lesser Antilles; (b) a geoidal *low* of −46 meters in the eastern Pacific Ocean area off Baja California, and (c) a geoidal *high* of +24 meters off the west coast of South America and centered at about 20° South latitude, 72° West longitude. There were thus three new areas of geoidal anomaly defined, as well as changes in magnitude for the anomaly areas defined earlier, and in three cases significant changes in location.

Figure 4 is an analysis of doppler tracking data by Guier and Newton (1965) using five satellites, and although there is excellent agreement with many of the features shown in Figure 3 there are still points of difference. There is agreement as to the location and magnitude of the *low* in the Indian Ocean, the *high* in the Solomon Islands region, the *high* between South Africa and Antarctica, the *high* along the west coast of South America, and the *low* off Baja California. However, the *low* in the western Atlantic region is shifted northward to off the Georgia-Carolina coast of the United

FIG. 3. Geoid based on optical data for eleven satellites (Izsak, 1967).

FIG. 4. Geoid based on doppler data for five satellites (Guier and Newton, 1965).

States and is shown to have a value of —70 meters, which makes it comparable in magnitude to that defined in the Indian Ocean. In addition Guier and Newton's map defines two anomalous areas that are not present on Izsak's map. There is a negative closure of —22 meters in the western North Pacific region centered at about 45° North latitude, 175° East longitude, and a positive closure of +60 meters south of Japan centered at about 25° North latitude, 140° East longitude.

Another recent geoidal map is that published by Anderle (1967) based on doppler tracking data. This is shown in Figure 5. Although Figure 5 has many points in common with both Figure 4 and Figure 3 as regards the basic pattern of *highs* and *lows,* there are significant differences in the magnitude of the anomalies, in some cases their shape, and in others the location of their centers.

As pointed out by Thomas (1967) in connection with these differences in geoidal maps, a basic problem in resolving the geoid from satellite data is the differences in procedures used by different investigators in deriving the coefficients of C_{nm} and S_{nm}. To quote Thomas, "There are almost as many variations in actual procedures as there are investigators in the field." However, despite these differences and as suggested by Figures 3, 4, and 5, there is a remarkable degree of similarity in results obtained recently. King-Hele (1967) has attributed this to the fact that the values for the complete potential of the gravitational field are more important than the values of individual coefficients. Sets of coefficients which look rather different may give very similar gravity fields. Also, as pointed out by King-Hele (1967) in regard to the reality of the anomalous areas of geoidal height and gravity
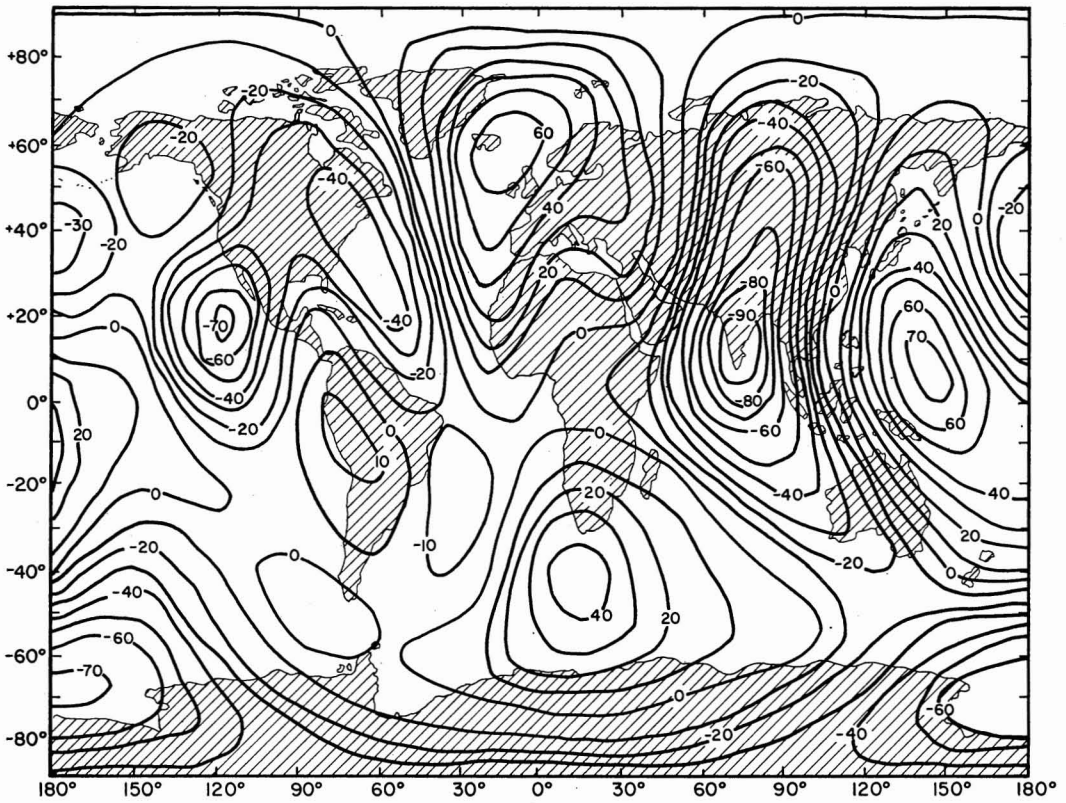
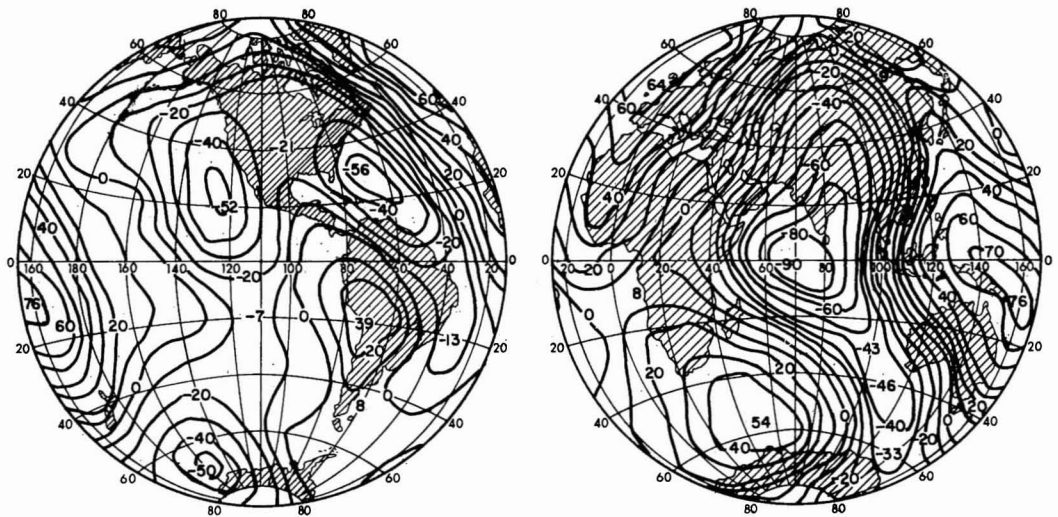FIG. 5. Geoid based on doppler data with f=1/298.3 (Anderle, 1967).

FIG. 6. Geoid based on the combination of satellite and gravity data referred to an ellipsoid with f=1/298.25 (Kaula, 1966).
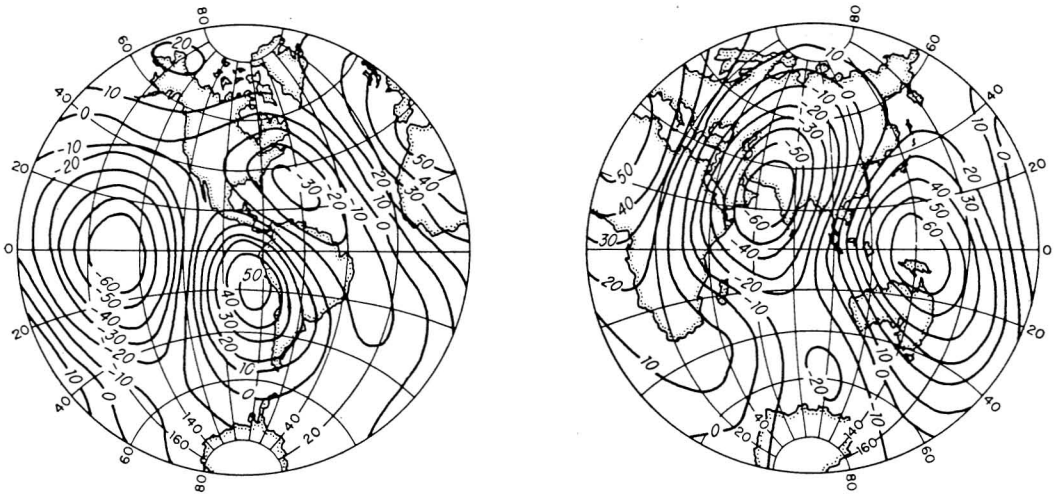
FIG. 7. Geoid based on gravity data only and referred to an ellipsoid with f=1/298.24 (Uotila, 1962).

defined by orbital analysis, it may be that the higher degree coefficients not evaluated are quite large and that their neglect constitutes a major source of error. The gravity comparisons, however, do not substantiate this concern.

Inclusion of surface gravity data in conjunction with satellite data in the analysis appears to make little difference in the anomaly pattern obtained. For example, compare Figure 6 derived by Kaula (1966) using satellite and surface gravity data with Izsak's (1967) map,

Figure 3. There are differences in magnitude of the geoidal undulations, but the number and location for the centers of anomalous geoidal height are nearly identical. The only point of difference is a negative closure of —50 meters centered off Antarctica at about 70° South latitude, 155° West longitude. That this high degree of agreement is not a consequence of the weight given the satellite data and the paucity of surface gravity data in the oceans covering approximately two-thirds of the
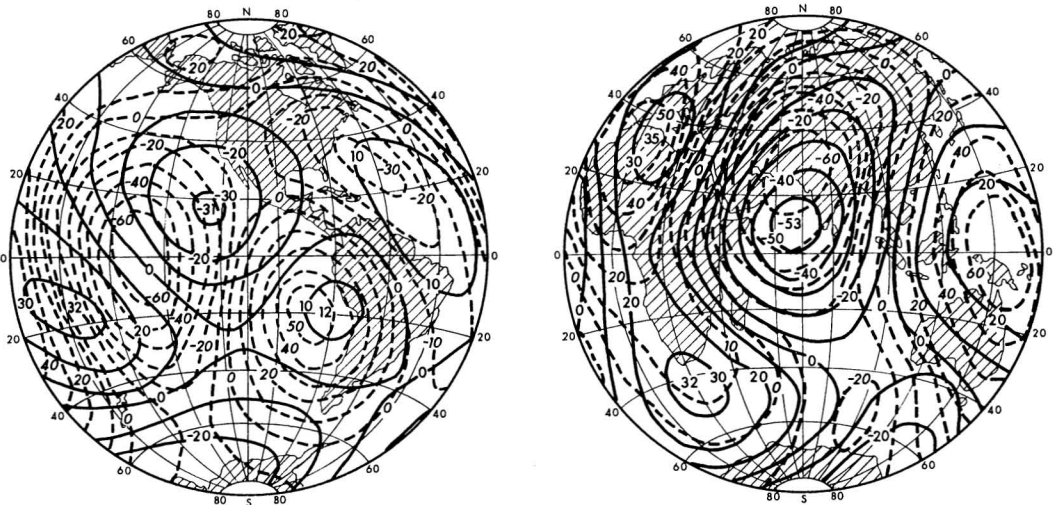
FIG. 8. Comparison of gravity and satellite-derived geoids (Thomas, 1967). ———— Satellite geoid (Izsak); – – – gravity geoid (Uotila).

WESTERN HEMISPHERE   EASTERN HEMISPHERE

FIG. 9. Comparison of gravity- and satellite-derived geoids (Kaula, 1966). ——— Gravimetric geoid; – – – satellite geoid.

Earth's surface is brought out by Figure 7, which is the geoidal map derived by Uotila (1962) using only surface gravity data and a satellite-derived reference ellipsoid whose flattening is 1/298.24. Despite the severe limitation under which Uotila was operating in terms of gravity coverage, it is to be noted that there is agreement as regards the *high* in the New Guinea-Solomon Islands region, the *low* in the Indian Ocean, the *low* off the eastern coast of North America, and the *high* off the Pacific coast of South America. Although Uotila's map defines a *low* off Antarctica it is at about 90° East longitude rather than 155° West longitude. Similarly the *high* shown on Kaula's map off the British Isles is displaced on Uotila's map to the vicinity of Tunisia in North Africa, and the *low* shown in the east Pacific region

FIG. 10. Geoid based on Kozai's and Gaposchkin's coefficients (Khan and Woollard, 1968a).

off Baja California in Figures 3, 4, and 5 is displaced to the Equator at about 150° West longitude. The most marked change in pattern on Uotila's map, however, is the absence of the *high* between Africa and Antarctica. A graphic comparison of Uotila's results versus those of Izsak (1967) prepared by Thomas (1967) is shown in Figure 8. A similar representation of the gravimetric and satellite geoids as derived by Kaula (1966) is shown in Figure 9.

Khan and Woollard (1968*a*), in studying the sensitivity of the derived geoid to the coefficients for the zonal and tesseral harmonics used, prepared a series of geoidal maps using different sets of coefficients as derived by various investigators, and also made an analysis based on average coefficient values. Figure 10 is their map based on an ellipsoid where C_{20} and C_{40} coefficients coincide with the satellite-observed values, and computed using Kozai's (1964) zonal harmonic coefficients and Gaposchkin's (1966) tesseral harmonic coefficients up to 8th degree order. This map agrees with Figure 3 and Figure 5 as regards the location of the New Guinea-Solomon Islands *high*, the Indian Ocean *low*, the eastern North Atlantic *high*, the western Atlantic *low* off Georgia, the South American Pacific coast *high*, and the eastern Pacific *low* off Baja California,

but it disagrees in terms of the *high* between South Africa and Antarctica, which is missing, and in the inclusion of a *low* off western Australia, a *high* just north of the Equator at 180° longitude and a *high* at about 30° South latitude, 170° West longitude.

Figure 11 is a similar map computed using Smith's (1963, 1965) zonal harmonic coefficients and Guier and Newton's (1965) tesseral harmonic coefficients up to 8th degree order. This map exhibits the same basic pattern as Figure 10 except that a positive closure is introduced between South Africa and Antarctica and two small closures (+22 and −22 meters) are introduced in the central South Pacific region, and a positive closure of 12 meters is shown over the Falkland Islands off Argentina.

Figure 12 is similar to Figures 10 and 11 but computed using the zonal harmonic coefficients of King-Hele et al. (1965) and Anderle's (1966) coefficients for the tesseral harmonics. This map is similar in basic pattern to Figure 10 in that the New Guinea-Solomon Islands *high* is shown, as well as the Indian Ocean *low*, the North Atlantic *high*, the western Atlantic *low* off the coast of the United States, the South American Pacific coast *high*, the eastern Pacific *low* off Baja California, and the *low* in the western North Pacific off Japan.
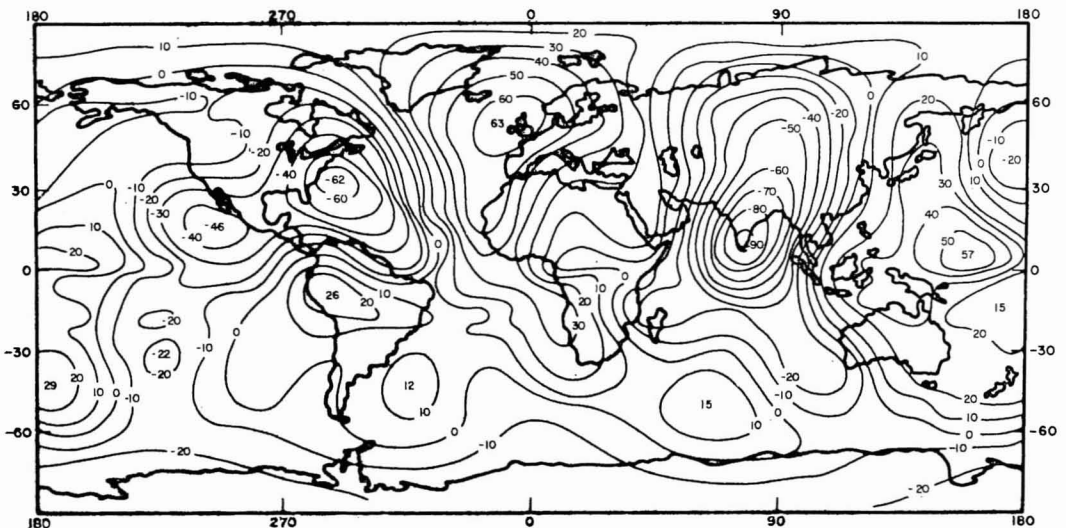

FIG. 11. Geoid based on Smith and Guier's and Newton's coefficients (Khan and Woollard, 1968*a*).
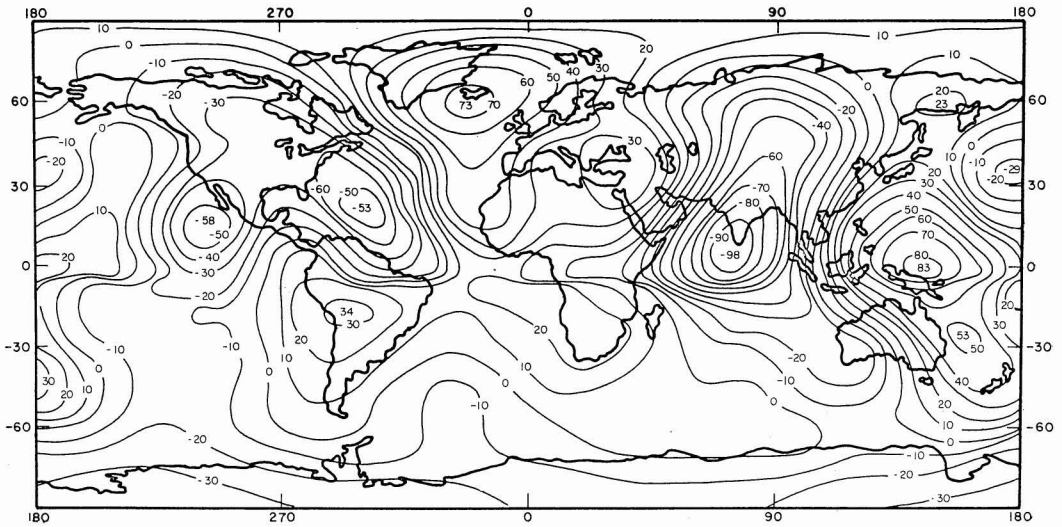
FIG. 12. Geoid based on King-Hele's and Anderle's coefficients (Khan and Woollard, 1968a).

The major point of difference lies in the occurrence of a *high* covering much of South Africa and the adjacent portion of the South Atlantic Ocean.

In Figure 13 the mean values for the zonal and tesseral harmonic coefficients used in preparing Figures 10, 11, and 12 were used. This map shows a pattern that incorporates all of the anomalous elements that were brought out in the other three maps.

Figures 10, 11, and 12 were each based on a slightly different reference ellipsoid as defined by the satellite data for the C_{20} and C_{40} terms, but this was not critical, as the spread in coefficient values was small, as is shown in Table 1 and Table 2. The effect of using the international reference ellipsoid with a polar flattening of 1/297 is shown in Figure 14 which was computed using the same mean coefficients as were used in deriving Figure
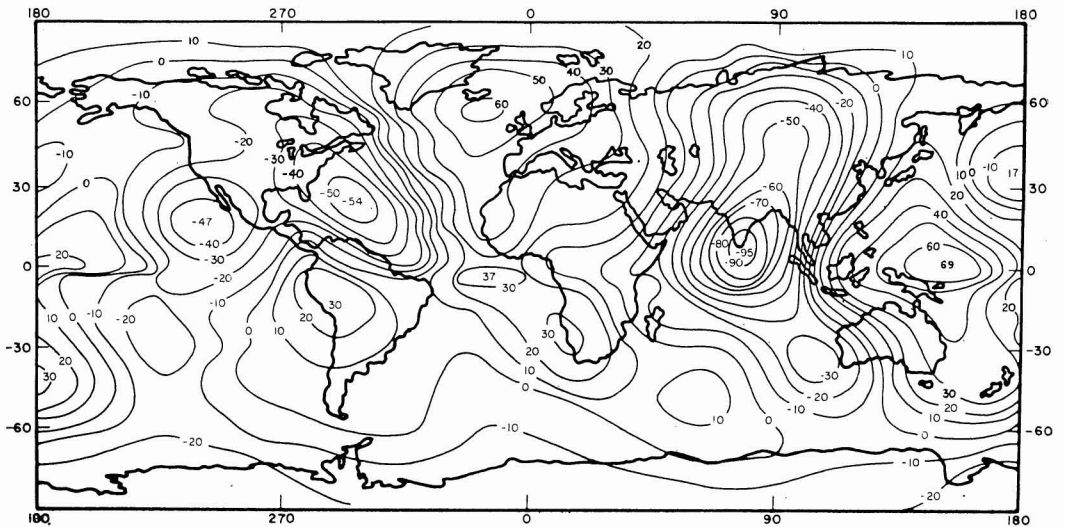
FIG. 13. Geoid based on mean coefficients (Khan and Woollard, 1968a).

TABLE 1

NORMALIZED ZONAL HARMONIC COEFFICIENTS C_{n0} OF THE GEOPOTENTIALS, IN UNITS OF 10^{-6}

n	SMITH (1963, 1965)	KOZAI (1964)	KING-HELE ET AL. (1965)
2	−484.172	−484.174	−484.172
3	0.923	0.963	0.967
4	0.567	0.550	0.507
5	0.054	0.063	0.045
6	−0.202	−0.179	−0.158
7	0.077	0.086	0.114
8	0.112	0.065	−0.107

13 in which the flattening of the reference ellipsoid is very nearly 1/298.25. As seen, use of the international reference ellipsoid results in much more pronounced geoidal height anomalies and gradients, with a pronounced east-west "grain" to the contours. With a polar flattening of 1/298.25 there is an apparent north-south "grain" to the contours, and, in general, marked agreement with the anomaly pattern defined in Figure 11. These results are substantiated by the studies by Köhnlein (1966), whose map of satellite-derived undulations of the geoid referenced to the satellite-derived

TABLE 2

NORMALIZED TESSERAL HARMONIC COEFFICIENTS OF THE C_{nm}, S_{nm} OF THE GEOPOTENTIAL IN UNITS OF 10^{-6}

| n	m	ANDERLE (1966) C_{nm}	S_{nm}	GUIER AND NEWTON (1965) C_{nm}	S_{nm}	GAPOSCHKIN (1966) C_{nm}	S_{nm}
2	2	2.45	−1.52	2.38	−1.20	2.38	−1.35
3	1	2.15	0.27	1.84	0.21	1.94	0.27
	2	0.98	−0.91	1.22	−0.68	0.73	−0.54
	3	0.58	1.62	0.66	0.98	0.56	1.62
4	1	−0.49	−0.57	−0.56	−0.44	−0.57	−0.47
	2	0.27	0.67	0.42	0.44	0.33	0.66
	3	1.03	−0.25	0.84	0.00	0.85	−0.19
	4	−0.41	0.34	−0.21	0.19	−0.05	0.23
5	1	0.03	−0.12	0.14	−0.17	−0.08	−0.10
	2	0.64	−0.33	0.27	−0.34	0.63	−0.23
	3	−0.39	−0.12	0.09	0.10	−0.52	0.01
	4	−0.55	0.15	−0.49	−0.26	−0.26	0.06
	5	0.21	−0.59	−0.03	−0.67	0.16	−0.59
6	1	−0.08	0.19	0.00	0.10	−0.05	−0.03
	2	0.13	−0.46	−0.16	−0.16	0.07	−0.37
	3	−0.02	−0.13	0.53	0.05	−0.05	0.03
	4	−0.19	−0.32	−0.31	−0.51	−0.04	−0.52
	5	−0.09	−0.79	−0.18	−0.50	−0.31	−0.46
	6	−0.32	−0.36	0.01	−0.23	−0.04	−0.16
7	1	0.33	0.08	0.13	0.09	0.20	0.16
	2	0.35	−0.19	0.46	0.06	0.36	0.16
	3	0.32	0.04	0.39	−0.21	0.25	0.02
	4	−0.47	−0.24	−0.14	0.00	−0.15	−0.10
	5	0.05	0.02	−0.06	−0.19	0.08	0.05
	6	−0.48	−0.24	−0.45	−0.75	−0.21	0.06
	7			0.09	−0.14	0.06	0.10
8	1			−0.15	−0.05	−0.08	0.07
	2			0.09	−0.04	0.03	0.04
	3			−0.05	0.22	−0.04	0.00
	4			−0.07	−0.04	−0.21	−0.01
	5			0.08	0.00	−0.05	0.12
	6			−0.02	0.67	−0.02	0.32
	7			0.17	−0.07	−0.01	0.03
	8			−0.15	0.09	−0.25	0.10
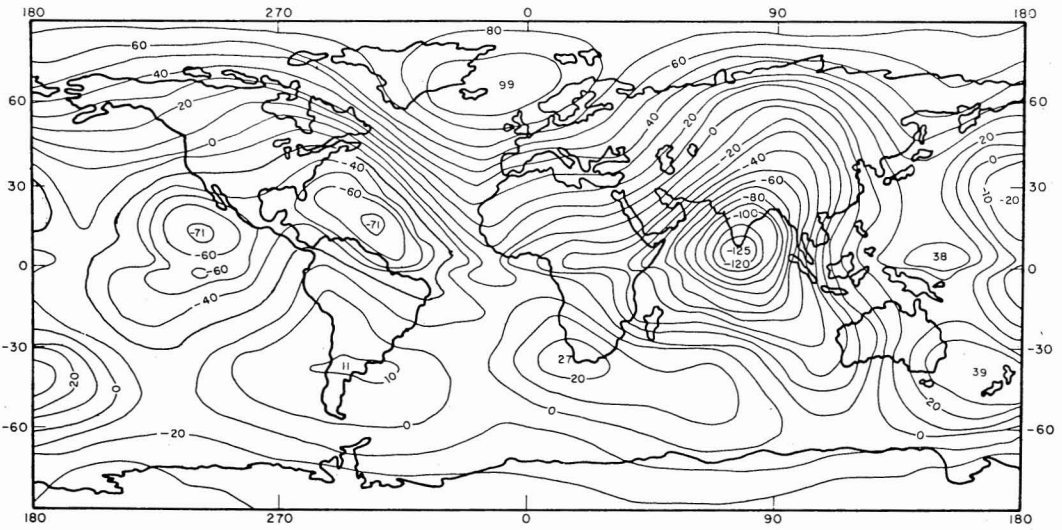
FIG. 14. Geoid based on mean coefficients and international ellipsoid (Khan and Woollard, 1968a).

ellipsoid is shown in Figure 15, and as referenced to the international ellipsoid, in Figure 1. Figure 17 shows the geoid based on the mean coefficients (Khan and Woollard, 1968a) and a reference figure whose zonal harmonics to the 8th degree are the same as the mean zonal harmonic coefficients referred to above.

The conclusions that can be reached from the above review are: (a) Starting with the first geoidal maps as derived by Kaula and by Guier

there has been a consistent pattern of a marked geoidal *low* associated with the Indian Ocean just south of India and a pronounced *high* in the New Guinea-Solomon Islands region. (b) As the number of satellites have increased having different orbital elements, other areas of anomalous geoidal height have been moved in position, as the western Europe *high* into the North Atlantic area, and new areas have been defined, as the *low* off the east coast of the
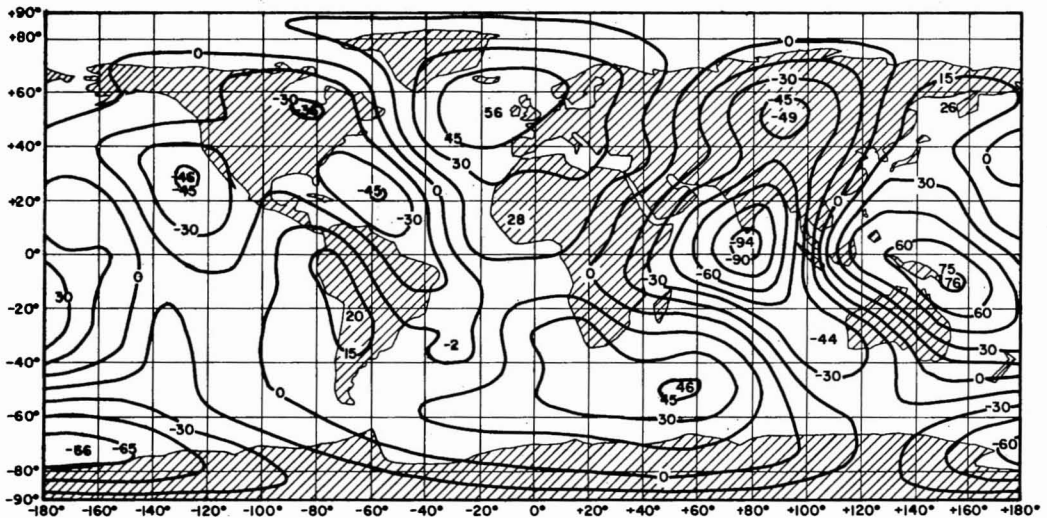
FIG. 15. Geoid with reference to a best-fitting satellite ellipsoid (Köhnlein, 1966).
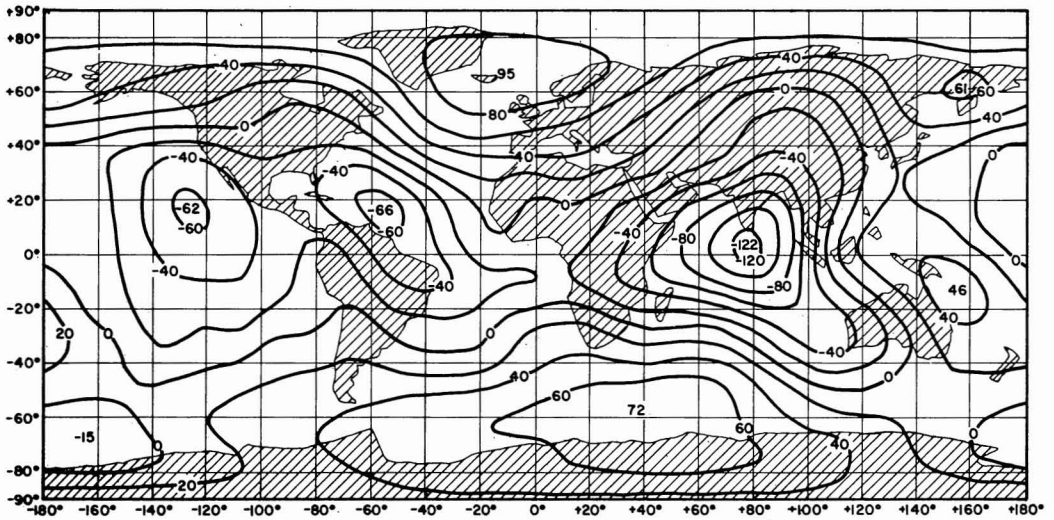
FIG. 16. Map of geoid with reference to the international ellipsoid (Köhnlein, 1966).

United States, the *high* between South Africa and Antarctica, the *low* off the coast of California, the *high* along the Pacific coast of South America, and the *low* in the North Pacific region between Hawaii and Japan. (c) Although there are differences in the zonal and tesseral harmonic values derived by different investigators, these differences do not critically affect the pattern of the derived geoid as long as the reference ellipsoid is similar, although they do make a difference in the magnitude of geoidal undulations. (d) Use of the international reference ellipsoid does make a significant difference in geoidal pattern. (e) The inclusion of surface gravity information does not significantly alter the geoidal pattern derived from satellite data alone.

One factor that should be borne in mind in
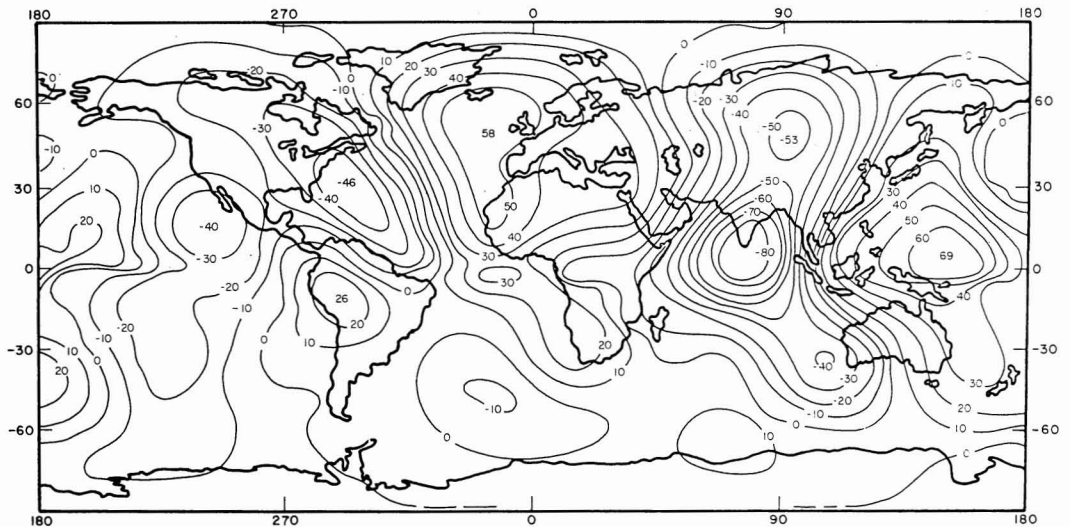
FIG. 17. Geoid based on mean coefficients and best-fitting satellite spheroid (Khan and Woollard, 1968a).

assessing these geoidal undulations is that the small-amplitude undulations having heights of the order 10 to 20 meters may be fictitious and a consequence of the mathematical "noise" inherent in making a spherical harmonic solution. Another factor, brought out by King-Hele (1967), is that the effect of neglecting the higher order harmonic terms is not yet clear. At this stage, it would appear that further refinement of the world geoidal map will depend on obtaining more comprehensive surface gravity information and incorporating these data with those from satellites, as has been done on a preliminary basis by Kaula (1967).

One is in Alaska and the Yukon Territory of Canada, where a negative closure is indicated while in the satellite solutions shown in Figures 11, 12, 13, and 17 only the trough of a low extends in that direction. Another is the negative gradient along the northern portion of the west coast of South America. Still another is the large closure area centered over Hudson Bay in eastern Canada. If it is assumed that Veis's adjustments of local data to those of a satellite-defined geoid with a polar flattening of 1/298.25 incorporate no errors, it is obvious that there are still problems to be resolved in relating the satellite data to the real Earth.

AGREEMENT WITH ASTROGEODESY

Although the geoid as defined from astrogeodetic measurements is only partially defined, the available data appear to substantiate the pattern of geoidal anomalies defined by satellite data. Figure 18 is a map of geoidal height variations as compiled by Veis (1966). As seen, the data are very incomplete, but the partial patterns—as in India, western Europe, the eastern United States, northeastern South America, the western United States, and the west coast of central South America—are all in agreement with that defined by the satellite data. However, there are points of difference.

GRAVITY RELATIONS

As indicated by Kaula (1966), a global harmonic and statistical analysis of gravimetric data using linear auto-covariance analysis gives a geoidal result that agrees with Guier and Newton's satellite-derived geoid within 30° for the location of the eight principal *highs* and *lows* on the worldwide geoid. The actual departures in pattern are shown in Figure 9, and the implication of the high degree of agreement obtained regarding the geoid using the two types of data is that the long wave length components of the surface gravity field can be derived from satellite data. Strange (1966),
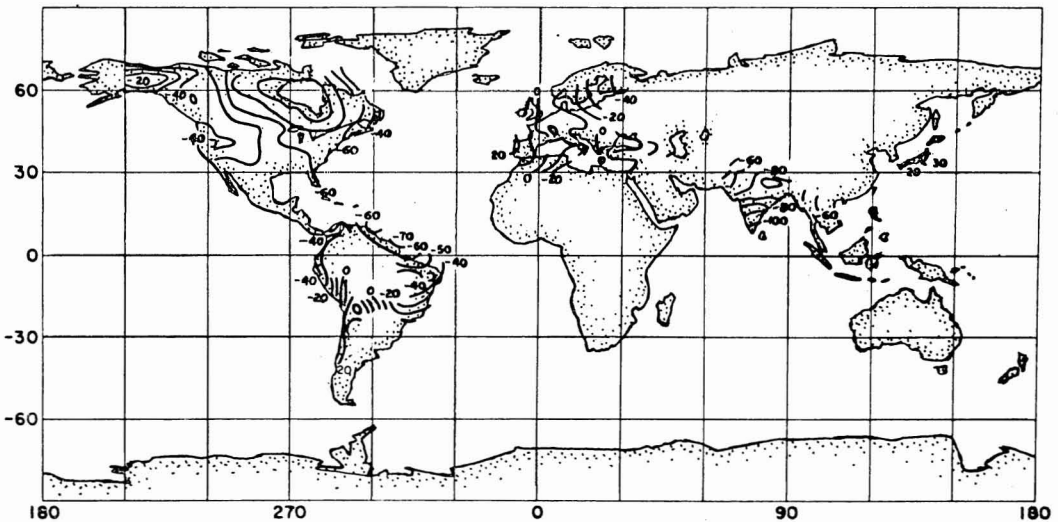

FIG. 18. The astrogeodetic geoid in the C6 system (a=6.378165, f=1/298.25) (Veis, 1966).

using the satellite results of Gaposchkin (1966), carried out a direct numerical comparison between satellite-derived and surface gravity data for those portions of the Earth where there were adequate surface data, and also made a determination of the extent to which satellite-derived free-air gravity anomalies are compatible on a worldwide scale with known relationships between surface gravity values and other physical parameters.

Figure 19 gives the results Strange obtained for a 6th degree representation of the anomalous surface gravity field in which the coefficients were computed using $5° \times 5°$ mean free-air anomaly values and assuming zero anomaly for those areas for which there were no data. The control was actually confined for the most part to the area lying between 15° and 135° West longitude and 20° and 50° North latitude. The size of this area and the control in the area was such that a 6th degree representation should not be in error by more than 4 to 8 mgal because of the lack of data outside the area. The 8th degree approximation of the anomalous gravity field derived by Strange using Gaposchkin's (1966) satellite results is shown as superimposed contours in Figure 19. Except for the area in the Indian Ocean and that off western Australia, the numerical agreement is better than 10 mgal. This degree of agreement can only be regarded as excellent, considering the limitations in surface gravity coverage and the fact that the two sets of contours represent different degrees of fit.

If a free-air gravity anomaly map based on Kaula's (1966) values using a combination of satellite and surface gravity data is considered (Fig. 20), it is seen that there are some significant differences in pattern as well as in numerical values from those derived by Strange (1966) (Fig. 19). The most significant differences are: (a) the positive values associated with the western North American and South American cordillera, which are 20 to 30 mgal more positive than those defined by Strange; (b) the pronounced area of positive anomalies exceeding +30 mgal extending from Greenland across the Norwegian Sea to Spitsbergen; (c) the pronounced local negative anomaly area extending across the Mediterranean Sea from Greece to Tripoli, North Africa; and (d) the positive anomaly area of about 20 mgal associ-

FIG. 19. Comparison of harmonic representation of surface gravity and satellite-derived free-air anomalies (Strange, 1966). ——— Satellite data; – – – surface gravity data.
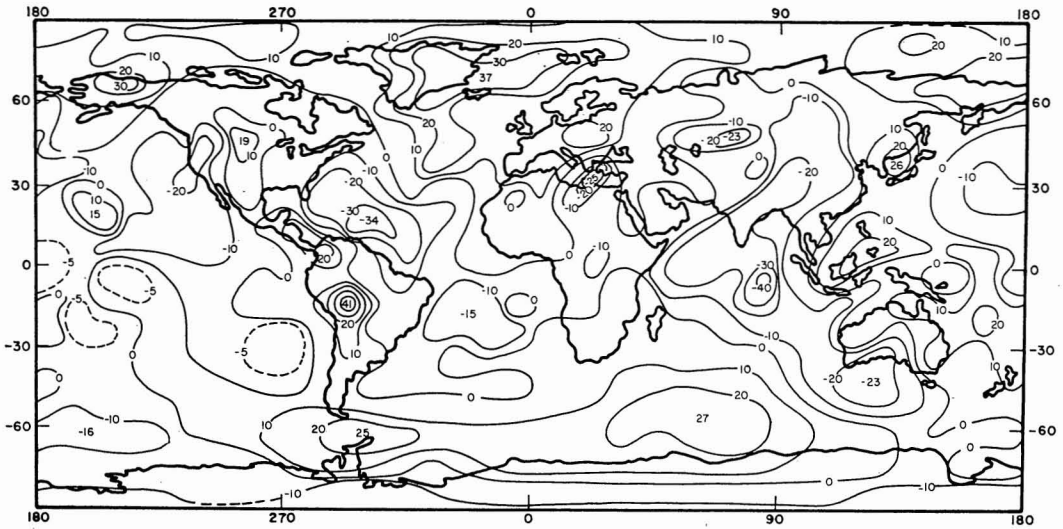
FIG. 20.   Free-air gravity anomaly map based on satellite and surface gravity data (Kaula, 1966).

ated with the Scotia Sea between South America and Antarctica. These differences, it is believed, can be attributed to the fact that Kaula used up to 14th degree coefficients and also incorporated surface gravity data in his solution. It should therefore be the better of the two.

Khan and Woollard derived a set of similar gravity maps from satellite data referenced to the International Gravity Formula, using com-

binations of Kozai's (1964) zonal and Gaposchkin's (1966) tesseral harmonic coefficients, Smith's (1963, 1965) zonal and Guier and Newton's (1965) tesseral harmonic coefficients, and the average of the zonal and tesseral harmonic coefficient values derived by various investigators. Their derived free-air gravity anomaly map based on the average coefficients is shown in Figure 21. As seen, the anomaly pat-
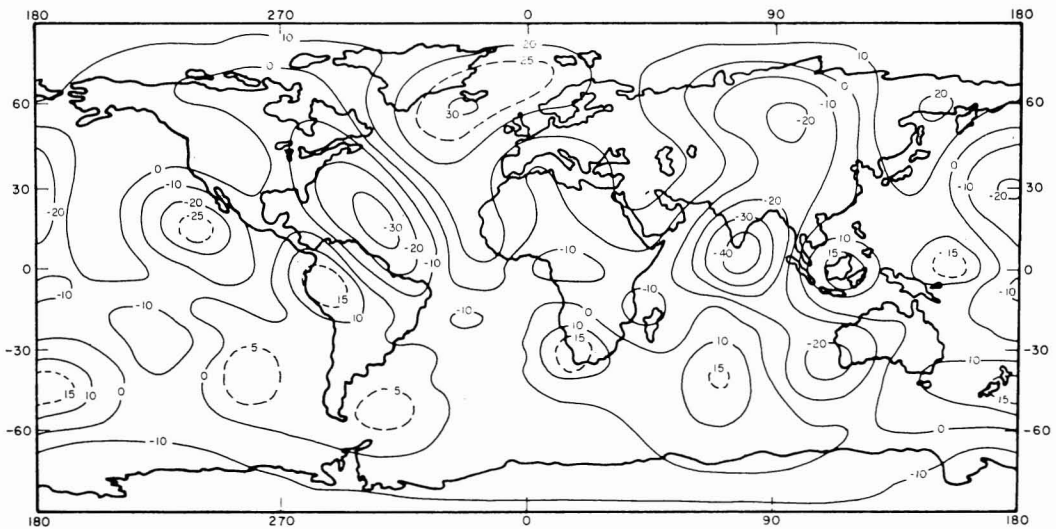
FIG. 21.   Free-air gravity anomaly map based on mean geopotential coefficients (Khan and Woollard, 1968a).
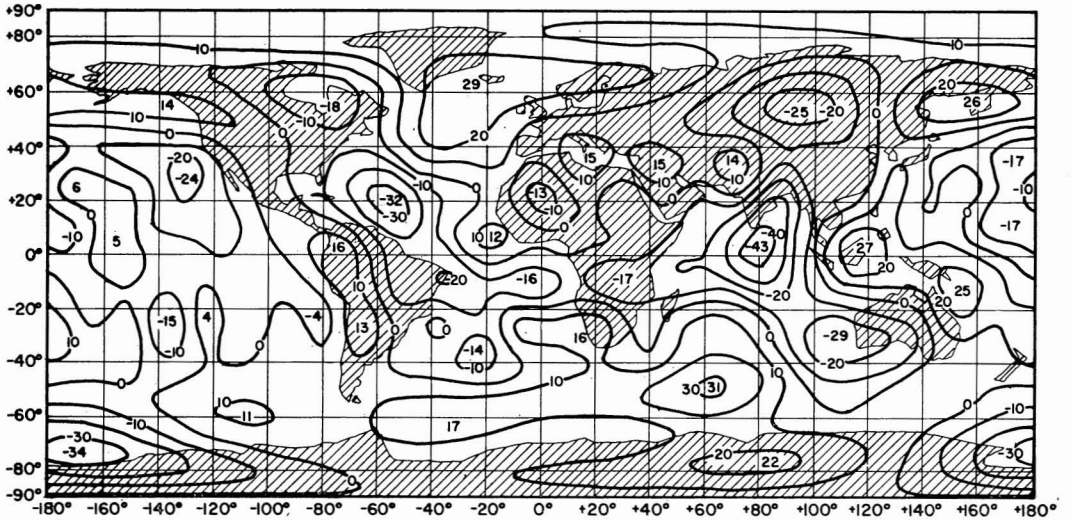
FIG. 22. Free-air gravity anomaly map based on optical data and on the international ellipsoid (Köhnlein, 1966).

tern and the amplitudes defined are somewhat different from those derived by both Strange and Kaula, although in general there is reasonable agreement with both. For example, the pattern of anomalies bears a closer agreement with Kaula than with Strange as regards the *high* extending across the Norwegian Sea and the disruption in pattern across Central America. On the other hand it agrees better with

Strange regarding the anomaly pattern associated with India and South Africa, and as regards the values associated with the cordillera of western South America.

One other gravity analysis of satellite data which should be considered is that by Köhnlein (1966). Köhnlein derived the surface free-air gravity anomaly field relative to the International Gravity Formula (Fig. 22) and also
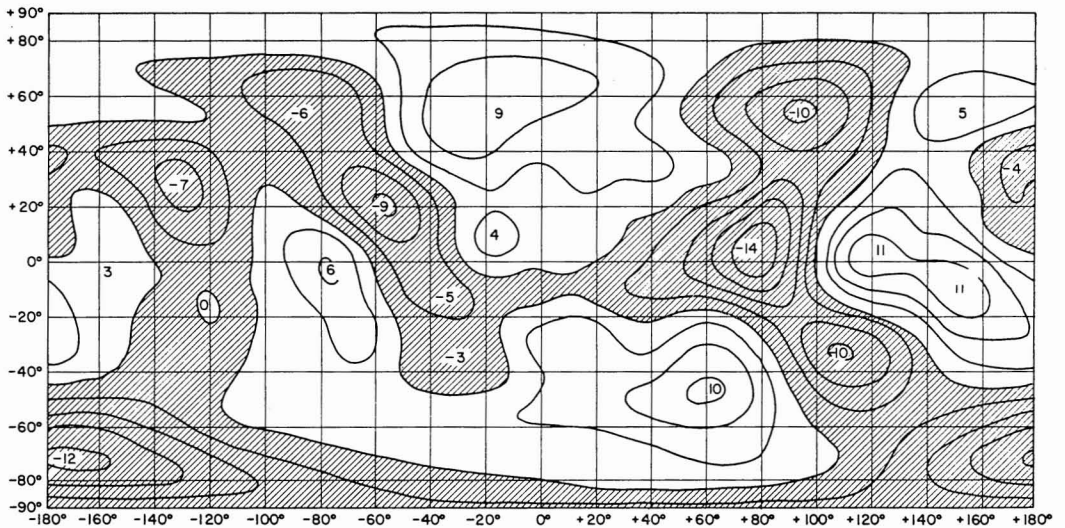
FIG. 23. Free-air anomaly field at 1000 km (after Köhnlein, 1966).

that at 1000 km elevation (Fig. 23) and at 10,000 km elevation. As seen, Köhnlein's derived surface gravity field has certain aspects in common with that derived by Strange that are not present in the Kaula and the Khan and Woollard maps, for example, the continuous gravity-positive area associated with the cordil-

lera of western North America and South America and the pronounced *low* shown over the Ross Sea area off Antarctica. It agrees closely, however, with the Khan and Woollard map for the *low* off the Pacific coast of North America, and with the Kaula map for the *high* in association with the Scotia Sea between South
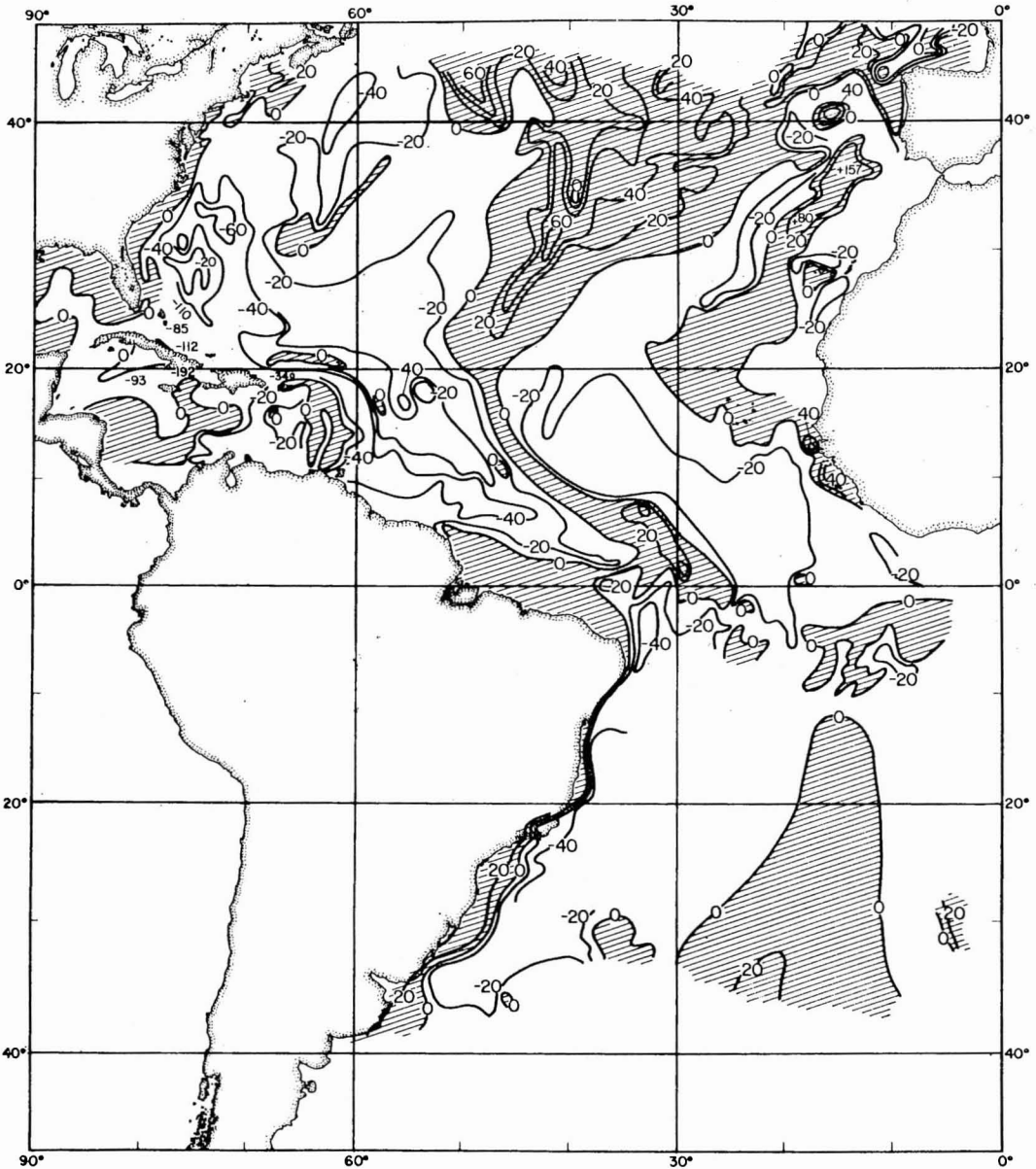
FIG. 24. Free-air gravity anomaly map, Atlantic Ocean area (Worzel, 1965). Contour interval=20 mgals.

America and Antarctica. It thus comes nearest to representing all the features brought out differentially on the other two maps and disagrees only on a few local anomaly areas, for example, the *high* of 15 mgal in the eastern Mediterranean Sea, where Kaula shows a *low* of —25 mgal, Khan and Woollard show no anomaly, and Strange, a local closure of +10 mgal.

Because a satellite senses only the integrated surface gravity field at satellite height, it is of interest to compare Köhnlein's map for the surface anomaly pattern (Fig. 22) with that derived for 1000 km elevation (Fig. 23). As seen, there is very little change in overall pattern, although the magnitude of the anomalies is reduced on the average by a factor of approximately 3.

As there is no way of identifying whether the gravity field sensed at height is related to that from a major mass anomaly at depth within the Earth or represents the integrated effect of a number of adjacent small mass anomalies located in the crust and upper mantle, there will always be a problem in relating the satellite-derived gravity field to that of the actual sur-

face gravity field. Certainly without harmonic representation of the surface data it is not possible to establish numerical agreement between the satellite-derived surface gravity field and the actual surface gravity field. Figure 24, for example, is the free-air anomaly map of the actual surface field for the North Atlantic region. As seen, the magnitude of the anomalies range from +60 mgal south of Greenland and over the Azores Islands to —200 mgal in association with the Puerto Rico Trench in the West Indies. Even with a 5° ✕ 5° representation of mean anomaly values, the range is from +40 mgal to —80 mgal, and with a 10° ✕ 10° representation, the range in mean anomaly values is from +30 mgal to —50 mgal. The range obtained by Strange using a 6th degree harmonic representation of 5° ✕ 5° actual surface data for this region (Fig. 19) was from +15 mgal to —15 mgal. His derived surface gravity anomaly field for the area ranged from +20 mgal to —20 mgal. Kaula's map incorporating both surface gravity data and satellite data (Fig. 20) gives a range of +20 mgal to —34 mgal for the same area. The map by Khan and
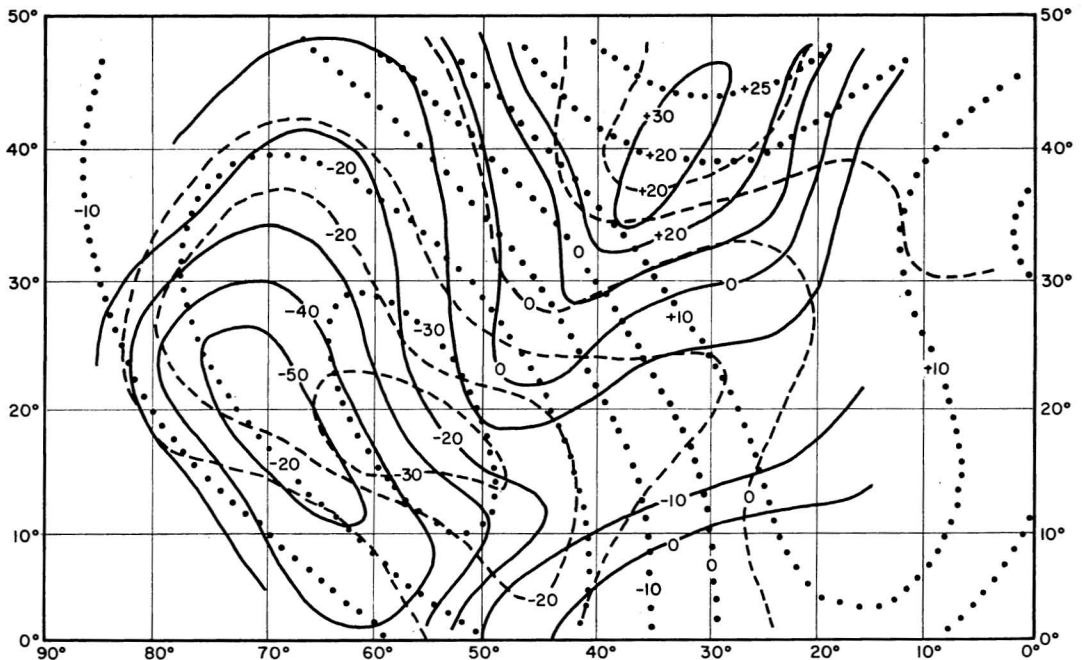

FIG. 25. Comparison of derived gravity field and actual free-air anomalies in the North Atlantic Ocean. ———— 10° ✕ 10° values; – – – Kaula; • • • Kahn and Woollard (1968*a*, after Khan and Woollard, 1968*b*).
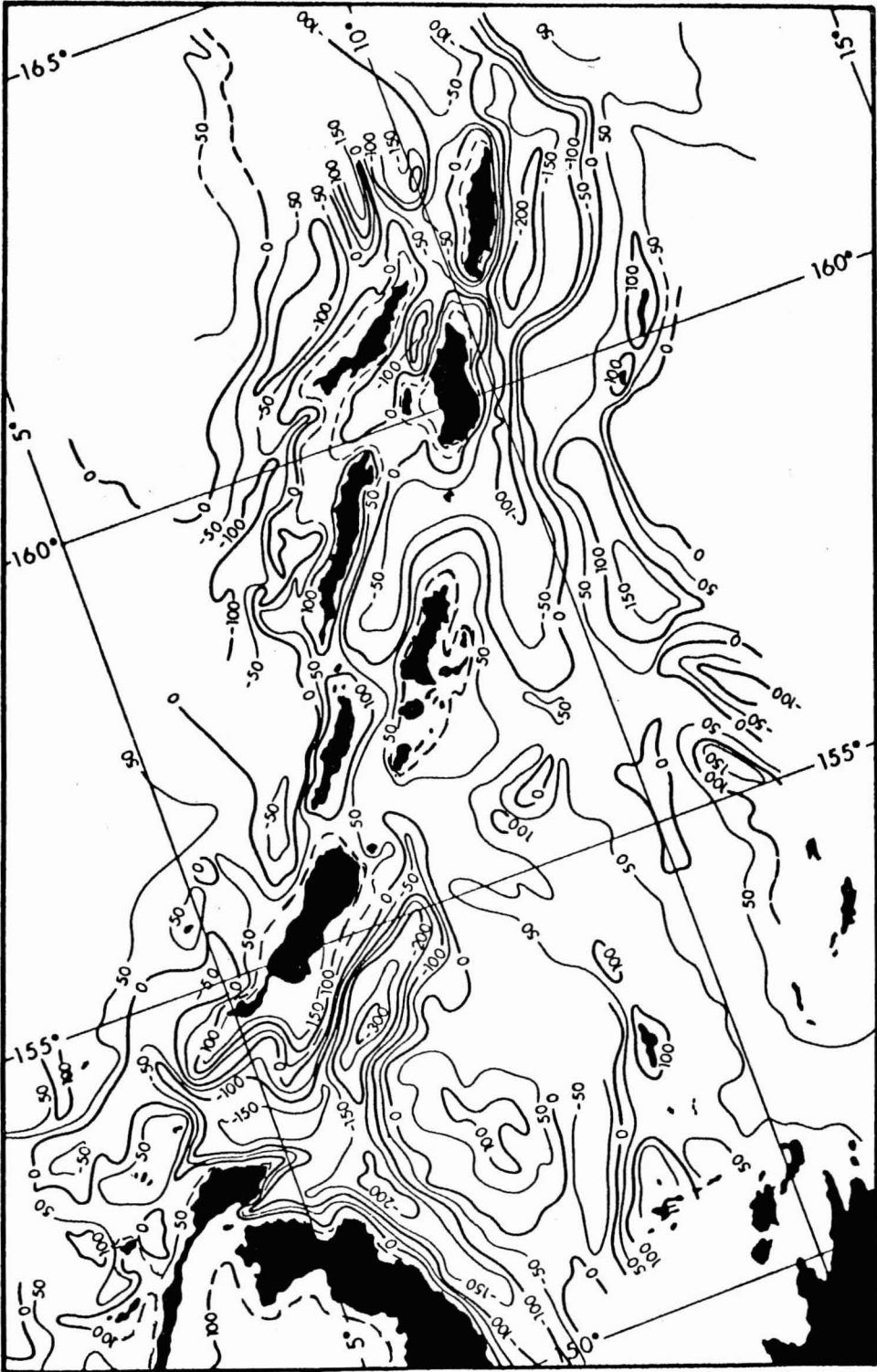
FIG. 26. Free-air gravity anomaly map of the Solomon Islands area (Woollard et al, 1967).

Woollard (Fig. 21) shows a range from $+25$ mgal to -30 mgal, and Köhnlein's map (Fig. 22) shows a range from $+25$ mgal to -32 mgal. As seen from Figure 25, which compares a $10° \times 10°$ mean anomaly representation of the actual field with that derived by Kaula and that by Khan and Woollard, the basic pattern defined by the satellite data is in good agreement as regards the North Atlantic *high,* but there is a 10° eastward shift in the location for the West Atlantic *low.* The major difference lies only in the numerical values for the anomaly areas. A test using $5° \times 5°$ mean anomaly values shows very similar results.

A basic problem yet to be resolved, therefore, is obtaining a realistic representation of the actual surface gravity field from satellite data. In areas having as complex a surface field as that found in the New Guinea-Solomon Islands region (Fig. 26), which is one of the major areas of anomalous geoidal height and where the satellite-derived gravity field does not exceed 25 mgal (Köhnlein solution) in any of the analyses to date, it may never be possible.

GEOPHYSICAL CORRELATIONS

As indicated in the introductory paragraphs, several attempts have been made to establish correlations between the areas of satellite-derived geoidal and gravitational anomaly and other geological and geophysical parameters. For the most part these have been statistical treatments which, as pointed out by Kaula (1967), "have been more noted for their variety than for their fruitfulness." There is a zero correlation with topography (ocean basins and continents), although as suggested by Strange (1966) there does appear to be a qualitative relation of positive satellite-derived free-air gravity anomalies to areas of Cenozoic to Recent volcanic and tectonic activity.

The most publicized statistical geophysical correlation with satellite data other than gravity is that of the inverse relation of derived geoidal and free-air gravity anomalies to heat flow (Lee and MacDonald, 1963; Wang, 1963). However, at the present time it appears that, where there are detailed data, there is a positive correlation between high heat flow values and excess gravity rather than with a deficiency in

gravity, for example the Rocky Mountains, the Mid-Atlantic Ridge, the East Pacific Rise, the Hawaiian Ridge, and the Solomon Islands-New Hebrides region. Von Herzen and Langseth (1965) conclude that in general heat flow in the oceans (the areas in which most satellite-derived geoidal and gravitational anomalies are found) is positive on the ridges (the areas of excess gravity) and negative in the basins (the areas of normal to deficient gravity). With specific reference to the Indian Ocean area of satellite-determined anomalous geoidal height and gravity, Von Herzen and Langseth show that, except for the Gulf of Aden which is a tectonic rift area characterized by excess gravity and high heat flow, there is no anomalous heat flow in the Indian Ocean using average $5° \times 5°$ values with either latitude or longitude between 20° North latitude and 50° South latitude and between 20° and 140° East longitude. This substantiates the conclusion reached by Strange (1966) regarding the relation of heat flow to gravity. Thus the one apparent authentic correlation that had been established appears to be at least in question. As the other correlations that have been attempted are even more tenuous, it cannot be said that any firm set of relations to satellite-derived data other than surface gravity have been established to date, and as indicated, it is only in the broadest sense of the pattern for mean $5° \times 5°$ and $10° \times 10°$ anomalies that this correlation exists.

Although the strong statistical correlation determined by Kaula (1967) between gravity and magnetism is verified in terms of magnetic anomaly fluctuations associated with the mid-ocean rises such as the Mid-Atlantic Ridge and the East Pacific Rise, the recent discovery of a pronounced pattern of magnetic polarity reversals in association with such features (Vine, 1966; Cox, Dalrymple, and Doell, 1967) introduces a question as to the validity of this correlation. Similarly, so long as it was thought that all abnormalities in crustal thickness other than that between the continents and ocean basins had gravity expression with a deficiency in gravity signifying abnormal crustal thickness and excess gravity signifying subnormal crustal thickness, it appeared that it might be possible to use the satellite-derived gravity field for defining areas of abnormal and subnormal crustal

thickness. It now appears (Woollard, 1962, 1966, 1968) that such a relation holds only for areas of tectonic displacement through block faulting of the crust or as a consequence of previous glacial loading, and that the normal relation is the reverse, with excess gravity characterizing areas of abnormal crustal thickness and a deficiency in gravity characterizing areas of subnormal crustal thickness.

The controlling mechanism in each case is the mean density of the crust, which is abnormal where the crust is thick and subnormal where the crust is thin. One consequence of this is that most major sedimentary basins, such as the Williston Basin covering much of eastern Montana and western North Dakota, are areas of excess gravity despite the thick section of included, relatively low-density sediments, and areas of geologic uplift such as Wisconsin are areas of subnormal gravity despite the fact that relatively high-density crystalline rocks are exposed at the surface. The factor controlling the mean density of the crust (Woollard, 1968) seems to be the presence and thickness of a high-density basal layer in the crust, and this in turn appears to be governed by the seismic velocity of the underlying mantle rocks. In general, where the seismic velocity of the mantle is high ($>$ 8.2 km/sec) the basal layer is well developed and the crust is abnormally thick for the surface elevation; where the mantle velocity is low ($<$ 8.0 km/sec) the basal layer is either thin or absent and the crust subnormal in thickness for the surface elevation. Although seismic velocity and density can usually be directly correlated, if there is a mineral phase transformation such as that between dunite and eclogite, or a change in Fe-Mg ratio, with a consequent change in mean atomic weight, the relations between velocity and density are reversed. It appears that some such mechanism is required to sustain nearly equal elevations and near-zero mean free-air gravity anomalies on the two sides of the Rocky Mountains, with a change from about 50 km in crustal thickness in the high plains area east of the Rocky Mountains to about 33 km in the Basin and Range area west of the mountains. This lack of regional change in gravity for these two areas of markedly different crustal thickness points up only too clearly the impossibility of using satellite-

derived data for this type of correlation. It also contrasts strongly with the direct correlation between surface gravity and satellite-derived gravity data for eastern Canada, where the crust appears to be out of isostatic equilibrium (too thick) as a consequence of former glacial loading that has now been removed. With time this anomaly should disappear.

From the above considerations it is clear that there is no simple set of relations relating the satellite-derived gravity field to other geophysical parameters of the Earth. The best utilization of satellite-derived geoidal and gravity data lies in their use for defining areas of anomalous gravity, whose significance can be established only through a program of ground-based study. It was with this objective that the first author initiated in 1962 a study of the geoidal *high* in the New Guinea-Solomon Islands region. This study is still in progress and to date has resulted in the gravitational mapping of parts of New Guinea, New Georgia, the Solomon Islands, the New Hebrides, the Solomon Sea, and the area to the north of the Solomon Islands. This has been supplemented by geologic mapping, magnetic mapping, nine measurements of crustal thickness using the seismic refraction technique, and several thousand miles of bathymetric and sub-bottom mapping using a spark source. The results show that the Solomon Islands have only recently emerged from the sea floor; they are active tectonically as evidenced by numerous earthquakes and active volcanoes; they appear to be at a locus of convergence of two oppositely moving crustal blocks, with deep trenches formed on their south side due to a flexure in the crust (Fig. 27), and with a fault boundary on their north side with over 2000 meters displacement and at whose foot lies a broad arch that has raised the sea floor nearly 1000 meters at its crest. While the gravity survey of the Solomon Islands region alone sufficed to show why this area should appear as an anomalous area of gravity as sensed by a satellite (over two-thirds of the area studied, embracing some 75 square degrees of latitude and longitude, is characterized by positive free-air anomalies averaging about +60 mgal), it was necessary to carry out the other studies to determine their cause. In contrast to the ocean rises such as the Mid-Atlantic Ridge, which is
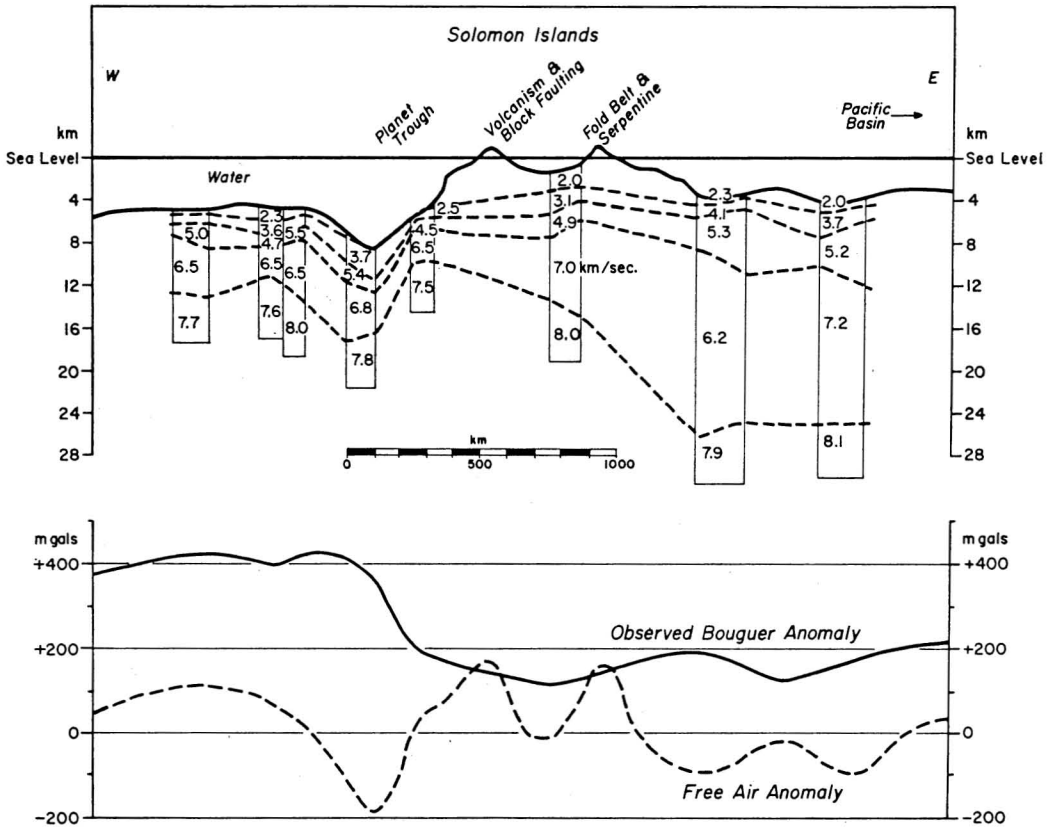
FIG. 27. Composite crustal section of the Solomon Islands region.

also an area of excess gravity and which appears to be the locus of crustal spreading, the Solomon Islands appear to mark a locus of crustal convergence that has resulted in uplift, volcanism, and intrusion from the mantle, giving an extensive series of high-density mafic rocks at the surface. Both types of area have volcanism in common, and both are characterized by local high heat flow and excess gravity, but the tectonic and other geophysical associations are radically different (Khan and Woollard, 1968b), as will be seen.

RELATIONSHIPS OVER THE NORTHERN MID-ATLANTIC RIDGE

The surface gravity field for the northern Atlantic region, whether specified by surface data or satellite-derived gravity data (see Fig. 24) shows a pronounced *high* that is centered

over the Mid-Atlantic Ridge. As this has been an area of intensive geophysical study by various investigators for a number of years, the geological and geophysical parameters are well known. The crustal and upper mantle structure as defined by seismic refraction measurements (Ewing and Ewing, 1959) show that off the flank the crust is normal in thickness ($\approx$ 5–5.5 km) and has a two-layer structure with 5.0 km/sec material making up approximately one-third of the crust, and material with a velocity of about 6.7 km/sec comprising the balance. The underlying mantle material is normal with a velocity of about 8.1 km/sec. However, as the axis of the ridge is approached the crust thickens both by depression of the crust mantle interface and as a consequence of the increase in surface elevation. As there is little change in the elevation below sea level for the base of the 5.0 km/sec upper layer (actually this surface
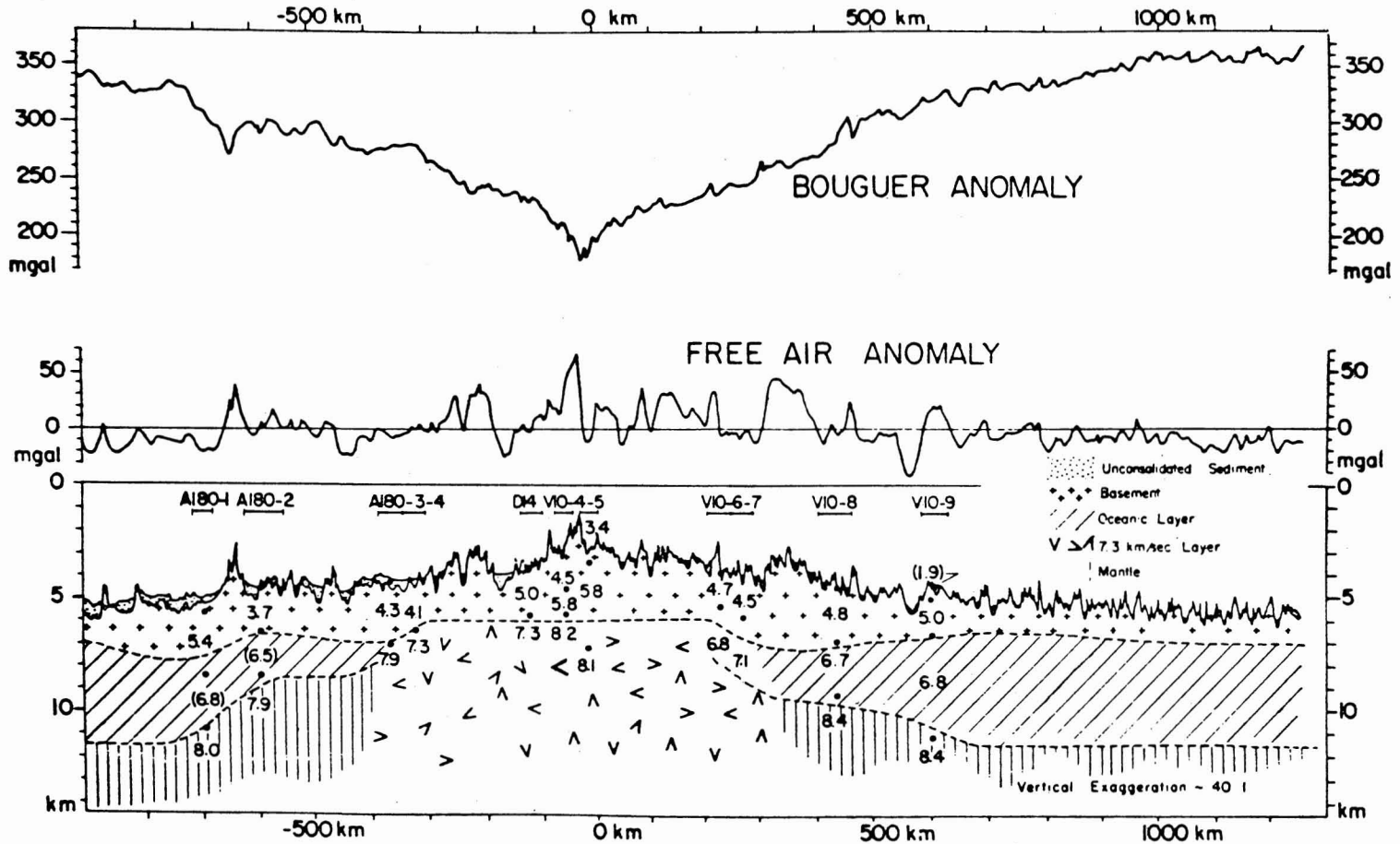
FIG. 28. Crustal section over the northern portion of the Mid-Atlantic Ridge (after Ewing, and Talwani and Worzel).

rises about 1.5 km beneath the axis of the Ridge), this layer thickens primarily in response to the increase in surface elevation. The 6.7 km/sec layer, however, thins as it is approached and is progressively replaced by material having a velocity of 7.3 to 7.5 km/sec. In the central area the 6.7 km/sec layer is completely missing, and either the mantle rock having a velocity of 8.1 km/sec is quite deep ($>$ 25 km below sea level) or the material with a velocity of 7.3 to 7.5 km/sec has also taken its place. Topographically, the axis of the Ridge is marked by a narrow graben and in this general area there is high heat flow, but on each side of this central area over the flanks of the Rise from about 200 to 600 km off the axis there is subnormal heat flow, as Von Herzen and Langseth (1965) have shown. The free-air gravity anomaly values, which average about $+30$ mgal over the entire width of the Ridge with values in excess of $+50$ mgal in the axis area, actually shows about a 50 mgal minimum in the Bouguer anomalies derived by allowing for the mass deficiency of the water column (see Fig. 28). As shown by Talwani, Heezen, and Worzel (1961), if the 5.0 km/sec upper layer of the crust is assumed to have a density of 2.6 gm/cm^3, and a density of 3.15 gm/cm^3 is assumed for the underlying material with a velocity of 7.3 to 7.5 km/sec, the mantle depth (assuming normal mantle material at depth with a density of 3.4 gm/cm^3) would have to extend down to at least 28 km beneath the axis of the Ridge.

This picture of crustal structure beneath the Mid-Atlantic Ridge, however, differs from that defined for the East Pacific Rise, which is believed to be of similar origin, on the basis of its topographic expression and pattern of heat flow anomalies. Here Menard (1964) showed that there is actual thinning of the crust beneath the Rise, and although subnormal mantle velocities of 7.5 to 7.6 km/sec were obtained, they are confined to the axial area where there is high heat flow.

It may well be that there is no *typical* pattern of geophysical relationships associated with the rises, other than of heat flow, restricted seismicity, and magnetic anomalies. Although one would expect similar gravity and crustal relations if the rises are loci for crustal spreading, as is strongly suggested by the symmetrical pattern of magnetic anomalies which now correlate with periods of reversals in the Earth's magnetic field (see Vine, 1966; Cox et al., 1967), the fact remains that no consistent gravity pattern has yet been established except in terms of the relative change in gravity. Even more disturbing—from the standpoint of establishing the significance of the satellite-derived gravity field—there is no apparent consistent relation to a given type of tectonic feature. Certainly the relationships found in the Solomon Islands area[3] differ radically from those found in the North Atlantic, although both have similar expression in the satellite-derived gravity field. The explanation may be that the mass anomalies sensed by the satellite have a deep-seated source, and hence any apparent correlation with surface features is purely fortuitous. It may be that a variety of tectonic features may have the same gravity expression, and it may be that, although a tectonic feature once formed has a long life, the causative phenomenon was of short duration. In this case, if the phenomenon influenced gravity, the gravity effect would disappear with time. This might explain, for example, why satellite-derived gravity data show an inconsistent relation to the oceanic rises with strong expression in the North Atlantic, none or only weak expression in the equatorial Atlantic region, and only a relative change (minus to plus values) over the East Pacific Rise, which, as was shown, has a markedly different set of crustal relations from those found in association with the Mid-Atlantic Ridge.

MAXIMUM DEPTH OF SOURCES FOR SATELLITE GRAVITY ANOMALIES

That the satellite-defined gravity anomalies are probably not of deep-seated origin (1000 km) can be shown by constructing anomaly profiles along parallels of latitude and analyzing the individual anomalies as to the maximum depth from which they can originate. Figure 29 shows profiles at 60°N, 30°N, the Equator, 30°S and 60°S latitude based on the gravity anomaly map prepared by Khan and Woollard (Fig. 2 in Khan and Woollard, 1968b). For purposes of analysis a regional base line has been superimposed, and the anomaly field ex-

---
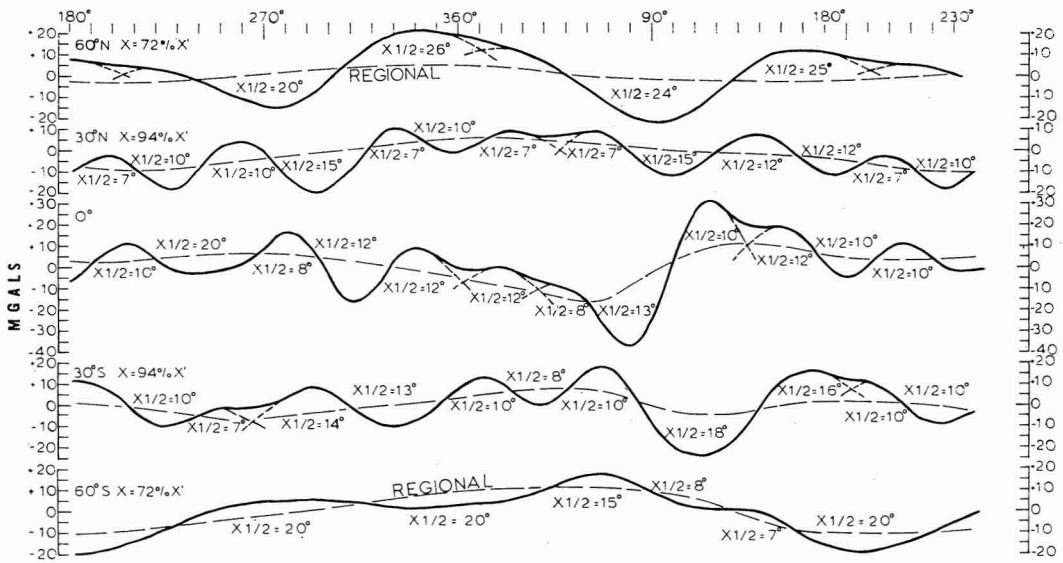
[3] See Khan and Woollard (1968b).

FIG. 29. Satellite-derived gravity profiles at 60°N, 30°N, the Equator, 30°S, and 60°S latitude (Khan and Woollard, 1968b).

amined as to whether a single or composite mass anomaly is depicted. As seen from Figure 29, all of the anomalies are either circular or elongate in plan. The circular ones can be thought of as originating from a mass having the general form of a sphere, a disc, or a vertical cylinder. The elongate anomalies can be thought of as originating from a body having the form of a vertical tabular body, a horizontal tabular body, or a horizontal cylinder. Depending on the geometry of the body and its orientation, there is a definite relationship between the half-width value (half the width of the anomaly at half-amplitude value) and the depth to the center of the disturbing mass. This is independent of the density contrast which affects only amplitude. As the maximum depth will be associated with those forms having a maximum concentration of mass (sphere and horizontal cylinder), the profiles were analyzed only in terms of these two mass distributions. The depth to half-width value relations for a sphere are $Z = 1.305(X \frac{1}{2})$ and for a cylinder $Z = 1.0$ $(X \frac{1}{2})$ where $X \frac{1}{2}$ is the half-width value. The depth value (Z) in each case is the depth to the center of the mass. The depth to the top of the mass will depend upon the radius of the body, which in turn is governed by the density

contrast involved. The amplitude (g_z) for a horizontal cylinder is

$$g_z = 2 \, \pi\gamma\delta \, R^2 \cdot \frac{Z}{Z^2 + X^2}$$

where γ is the gravitational constant, δ is the density contrast; R is the radius of the body, Z is the depth to the center of mass, and X is the distance from a point directly over the center of mass. For a sphere, the expression is

$$g_z = \frac{4 \, \pi\gamma\delta \, R^3}{3} \cdot \frac{Z}{(Z^2 + X^2)^{3/2}}.$$

With the above two expressions, the observed half-width value $(X \frac{1}{2})$, the areal plan of the anomaly, and the height of the satellite specified, it is possible, using a reasonable estimate of δ, to determine the probable depth to the top of a disturbing mass. The basic assumption here is that the anomaly does not represent the integration of several shallow-seated mass anomalies as sensed at satellite height, but rather originates from a single source at depth. In other words, such an analysis assumes a single mass anomaly and we have deliberately assumed maximum depth conditions.

As shown in Figure 29, the half-width values range from 7° to 26°, with the shallower values predominating. If allowance is made for

the fact that the profiles are taken from a map on a mercator projection, the maximum half-width value is about 20°. Although an earth-orbiting satellite has a height corresponding to 4° of latitude, this should not have to be considered since the half-width value defined at the Earth's surface is a projected value. This conclusion is supported by the similarity in areal dimensions of harmonic representations of the actual surface gravity field as well as by average representations of the surface field for areas of 5° $\times$ 5° and 10° $\times$ 10° size (see Figs. 19 and 25). As the density contrast (δ) is not known, it is useful to examine the depth range 7° ($\approx$ 700 km) to 20° ($\approx$ 2000 km) in terms of what is known from seismic data concerning the internal structure of the Earth. We can immediately dismiss the "M" discontinuity which lies in the depth range 11 to 70 km. However, the seismic low-velocity zone at around 110 to 150 km might be a possible locus of mass inequality. Another is the 460 km seismic discontinuity, and another, the 1000 km seismic discontinuity. The core, at a depth of 2900 km, would appear to be too deep, as the half-width value depths are to the center of the mass and not to the upper surface of the mass anomaly. Most of the anomalies, if they are indeed from a deep source and correlate with seismic discontinuities, are at no greater depth than that of the 460 km discontinuity, but could be associated with the seismic low-velocity zone (110 to 150 km). Even at these relatively shallow depths, for the magnitude of the anomalies (10 to 20 mgal for 10° $\times$ 10° size areas) and the implied size of the bodies (R = 250 to 550 km), the density contrasts indicated are quite small and of the order of .01 to .02 gm/cm³. For anomalies with a half-width of 20° that might be related to the 1000 km discontinuity, if R = 1000 km and the anomaly is of the order of 30 mgal, the density contrast would still be only about .04 gm/cm³, which is an order of magnitude smaller than that associated with the "M" discontinuity defining the base of the Earth's crust.

CONCLUSION

It is clear that all satellite solutions, whether based on optical or doppler data, are now giving consistent relationships concerning the geoid and the Earth's gravity field, and that there will be few refinements except through the inclusion of more surface gravity data as it becomes available. It is also clear that at present the state of our geophysical knowledge concerning the Earth and its surficial and near-surface structures is so incomplete that no consistent pattern of relationship can as yet be established.

While the satellite program has thus contributed significantly to the advance of dynamic geodesy, and, through the present program of interconnections of widely separated points on the Earth's surface, will result in a similar advance in geometric geodesy, it has also contributed significantly to the advance of geophysical knowledge. Some contribution has been through direct applications as have been attempted in relating the satellite-derived gravity field to magnetism, heat flow, and other Earth parameters, but to the present, more important contribution has been through the specification of areas for comprehensive geophysical and geological investigation. Once an understanding is had of what factors control the gravity field in these areas, and if in fact there is an actual near-surface control, it will be possible to capitalize on the full scientific potential of the satellite data. To date, geophysical observations in any detail are available for only three of the eight areas of anomalous geoidal height and gravity defined by the analyses of satellite orbital observations, and even in these three areas the data are far from complete. Over the Mid-Atlantic Ridge the seismic measurements do not define the location of the mantle, and the gravity solution may or may not be correct. For the Indian Ocean, the data are incomplete in terms of the definition of the surface gravity field and measurements of crustal structure. In the Solomon Islands region only, a good start has been made in these studies.

That the anomalies are not related to mass inhomogeneities associated with the Earth's core can be demonstrated by quantitative analyses of the anomaly half-width values. However, it is not possible at this time to say whether they originate from seismically defined discontinuities in the Earth's structure at depths ranging from 150 to 1000 km, or whether they represent the intergration of near-surface mass anom-

alies associated with the crust and upper mantle. (Note: Figures 10 through 14, 17, 20, and 21 were computed in June 1966 on an IBM 7040 computer. A Subroutine FPT V-9 was used to suppress the overflow and underflow in the computations.)

LITERATURE CITED

ANDERLE, R. J. 1966. Determination of the Earth's geoid by satellite observations. U.S. Naval Weapons Laboratory Technical Report No. 2027, March 26, 1966.

———— 1967. Geodetic parameter set NWL-5E-6 based on doppler satellite observations. In: The use of artificial satellites for geodesy. Publication of the National Technical University of Athens, Greece, pp. 179–220.

BAUSSUS, H. G. 1960. A unified isostatic and statistical theory of gravity anomalies and its significance. Paper presented at the International Association of Geodesy, 12th Assembly, I.U.G.G., Helsinki, 1960.

COX, A., G. B. DALRYMPLE, and R. R. DOELL. 1967. Reversals of the Earth's magnetic field. Scientific American, vol. 216, pp. 44–54.

EWING, J. I., and M. EWING. 1959. Seismic-refraction measurements in the Atlantic Ocean basins, in the Mediterranean Sea, on the Mid-Atlantic Ridge and in the Norwegian Sea. Bulletin of the Geological Society of America, vol. 70, pp. 291–318.

GAPOSCHKIN, E. M. 1966. A dynamical solution for the tesseral harmonics of the geopotential and for station coordinates. (Abstract.) Transactions of the American Geophysical Union, vol. 47, p. 47.

GUIER, W. H. 1963. Internal report, Applied Physics Laboratory, Johns Hopkins University.

GUIER, W. H., and R. R. NEWTON. 1965. The Earth's gravity field as deduced from the doppler tracking of five satellites. Journal of Geophysical Research, vol. 70, pp. 4613–4626.

IZSAK, I. G. 1967. A new determination of non-zonal harmonics by satellites. In: The use of artificial satellites for geodesy. Publication of the National Technical University of Athens, Greece, pp. 221–229.

KAULA, W. M. 1963. A review of geodetic parameters. NASA TN D-1847.

———— 1966. Global harmonics and statistical analysis of gravimetry. In: Gravity anomalies: unsurveyed areas. Geophysical Monograph No. 9, American Geophysical Union, Washington, D. C., pp. 58–67.

———— 1967. Comparison and combination of satellites with other results for geodetic parameters. In: The use of artificial satellites for geodesy. Publication of the National Technical University of Athens, Greece, pp. 425–442.

KHAN, M. A., and G. P. WOOLLARD. 1968a. A review of the perturbation theory as applied to the determination of geopotential. Hawaii Institute of Geophysics Report No. HIG-68-1.

———— 1968b. Methods of analysis and comparison of geophysical data on a plane, with specific application to the Solomon Islands area. Hawaii Institute of Geophysics Report No. HIG-68-17.

KING-HELE, D. G. 1967. Review of dynamic methods for determining zonal harmonics in the Earth's gravitational potential. In: The use of artificial satellites for geodesy. Publication of the National Technical University of Athens, Greece, pp. 123–132.

KING-HELE, D. G., et al. 1965. The odd zonal harmonics in the Earth's gravitational potential. Planetary and Space Science, vol. 13, pp. 1213–1232.

KÖHNLEIN, W. 1966. The geometric structure of the Earth's gravitational field. In: Geodetic parameters for a 1966 Smithsonian Institution Standard Earth. Vol. 3. Smithsonian Astrophysical Observatory Special Report 200, Cambridge, Massachusetts, pp. 21–102.

KOZAI, Y. 1964. New determinations of zonal harmonic coefficients of the Earth's gravitational potential. Publication of the Astronomical Society of Japan, vol. 16, pp. 263–284.

LEE, W. H. K., and G. J. F. MACDONALD. 1963. The global variation of terrestrial heat flow. Journal of Geophysical Research, vol. 68, pp. 6481–6492.

MENARD, H. W. 1964. Marine geology of the Pacific. McGraw-Hill, New York.

RUNCORN, S. K. 1964. Satellite gravity mea-
surements and a laminary viscous flow model
of the Earth's mantle. Journal of Geophysi-
cal Research, vol. 69, pp. 4389–4394.

SCHEFFER, V. 1966. The European geoid and
its relations to geology. Geofisica E Me-
teorologia, vol. 15, nos. 1–2, pp. 23–29.

SMITH, D. E. 1963. A determination of the
odd harmonics in the geopotential function.
Planetary Space Science, vol. 11, pp. 789–
795.

——— 1965. A determination of the even
harmonics in the Earth's gravitational poten-
tial function. Planetary Space Science, vol.
13, pp. 1151–1159.

STRANGE, W. E. 1966. Comparison with sur-
face gravity. In: Geodetic parameters for a
1966 Smithsonian Institution Standard Earth.
Vol. 3. Smithsonian Astrophysical Observa-
tory Special Report 200, Cambridge, Massa-
chusetts, pp. 15–20.

TALWANI, M., B. C. HEEZEN, and J. L. WOR-
ZEL. 1961. Gravity anomalies, physiography,
and crustal structure of the Mid-Atlantic
Ridge. Publications du Bureau Central Sis-
mologique International, ser. A, facs. 22,
pp. 81–111.

THOMAS, P. D. 1967. Background on geodetic
principles and theories. Proceedings of First
Marine Geodesy Symposium, U.S.G.P.O.,
Washington, D.C., pp. 9–26.

UOTILA, U. A. 1962. Harmonic analysis of
world-wide gravity material. Publications of
the Isostatic Institute of the International
Association of Geodesy, vol. 39.

VEIS, G. 1966. Geodetic interpretation. In:
Geodetic parameters for a 1966 Smithsonian
Institution Standard Earth. Vol. 3. Smith-
sonian Astrophysical Observatory Special Re-
port 200, Cambridge, Massachusetts, pp.
1–14.

VINE, F. J. 1966. Spreading of the ocean floor.
Science, vol. 154, pp. 1405–1415.

VOGEL, W. 1960. Über Unregelmässigkeiten
der äusseren Begrenzung des Erdkerns auf
Grund von am Erdkern reflecktierten Erd-
bebenwellen. (Gerlands) Beiträge zur Geo-
physik, vol. 69, pp. 150–174.

VON HERZEN, R. P., and M. G. LANGSETH.
1965. Present status of oceanic heat-flow
measurements. In: Physics and chemistry of
the earth. Vol. 6. Pergamon Press, New
York. Pp. 365–407.

WANG, C. Y. 1963. On the distribution of
surface heat flow and second-order variations
in the external gravitational field. Smith-
sonian Institution Astrophysical Observatory
Report 134.

WOOLLARD, G. P. 1962. The relation of grav-
ity anomalies to surface elevation, crustal
structure, and geology. University of Wis-
consin Geophysical and Polar Research Cen-
ter Report 62–9.

WOOLLARD, G. P. 1966. Regional isostatic re-
lations in the United States. In: The Earth
beneath the continents. Geophysical Mono-
graph No. 10, American Geophysical Union,
Washington, D.C., pp. 557–594.

WOOLLARD, G. P. 1968. The interrelationship
of the crust, the upper mantle, and isostatic
gravity anomalies in the United States. In:
The crust and upper mantle of the Pacific
area, Geophysical Monograph No. 12. Amer-
ican Geophysical Union, Washington, D. C.,
pp. 312–341.

WOOLLARD, G. P., A. S. FURUMOTO, G. H.
SUTTON, J. C. ROSE, ALEXANDER MALA-
HOFF, and L. W. KROENKE. 1967. Cruise
report on the 1966 seismic refraction expe-
dition to the Solomon Sea. Hawaii Institute
of Geophysics Technical Report 67–3, 31 pp.

WORZEL, J. L. 1965. Pendulum gravity mea-
surements at sea, 1939–1959. John Wiley
and Sons, New York.